

On Reservoir Detection with Multichannel Transient EM Method in On-Shore and Off-Shore Environment

Zalina Dzhatieva, MTEM Ltd, Edinburgh, UK
Bruce Hobbs, MTEM Ltd, Edinburgh, UK
Anton Ziolkowski, MTEM Ltd, Edinburgh, UK
David Wright, MTEM Ltd, Edinburgh, UK
Craig Clarke, MTEM Ltd, Edinburgh, UK
John Linfoot, MTEM Ltd, Edinburgh, UK
Guangpin Li, MTEM Ltd, Edinburgh, UK

SUMMARY

The MTEM method demonstrated its abilities for a high resistive target such as hydrocarbons in both on-land and marine application. Since MTEM generates a variety of frequencies that gives a significantly better resolution in comparison with any DC or controlled source soundings. 1D approach for inverting multi-offset MTEM data is illustrated with the ability to determine gross features of the subsurface resistivity variations both laterally and with depth. We expect it will provide a reliable starting model for more complex 3D inversion schemes which is under development.

Keywords: Multi-Transient Electromagnetics, Multi-Offset inversion, monitoring hydrocarbons

INTRODUCTION

The multi-channel transient electromagnetic (MTEM) technique has proved effective at delineating and monitoring hydrocarbons (Wright, et al., 2002, Ziolkowski et al., 2005). The method works by injecting a transient current into the ground using a grounded wire source, and recording the potential difference, or electric field, between two receiver electrodes some distance, or offset, from the source. Any known transient signal can be used for the input current, including a straightforward step or a pseudo-random binary sequence.

The data examined in this paper were obtained in a demonstration survey over a reservoir in Canada in 2005. The objective of the survey was to delineate the top and lateral extent of the tar reservoir. The target depth was about 100 m. Provided no other information about the target made the survey effectively a blind test.

It has been proven (D. Wright, 2004) that in-line geometry of the multi-transient is more sensitive for resistor than the broadside one. In the field the signal

generated was a Pseudo Random Binary Sequence between two electrodes separated by the distance of 50 m and there were 20 receiver channels for each source position with in-line geometry.

MTEM METHOD

MTEM uses many source and receiver positions that allow to control the penetration depth. Offset to depth ratio with the factor of 2.5 is an indication of the depth to which the EM energy has penetrated. The current MTEM system uses pseudo-binary sequences for the source and has 40 live receiver channels.

1. Real time Acquisition

The MTEM transient allows the use of imaging techniques in the field to produce a preliminary resistivity map of the subsurface immediately the data is recorded.

We are able to relate the arrival time of the peak of the earth impulse response function to a pseudo-resistivity. This information is essentially independent of the absolute amplitude of the response and is therefore

independent of the amplitude information displayed in the common-offset sections. The pseudo-resistivity value is simply the resistivity of a uniform halfspace that has the same arrival time as the peak of the earth impulse response (as shown in Figure 1). The pseudo-resistivities are plotted in midpoint-offset coordinates, but with the offset scale divided by 2.5.

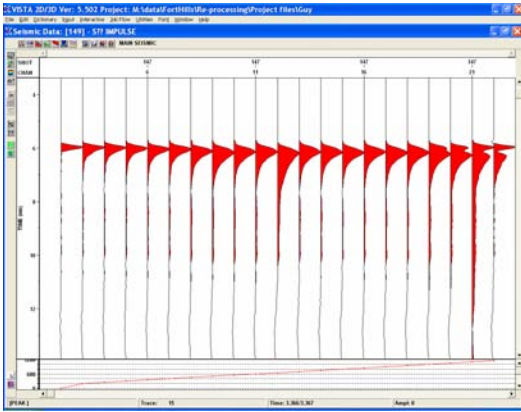


Figure 1. Impulse responses from resistive near surface. Earth Impulse response does not separate from the airwave ‘till longer offsets.

2. Step - On Inversion

Multi-Offset 1D Occam Inversion

After processing, MTEM data consist of impulse response functions for each source-receiver pair, which we demonstrate obey reciprocity. We integrate these to obtain step response functions.

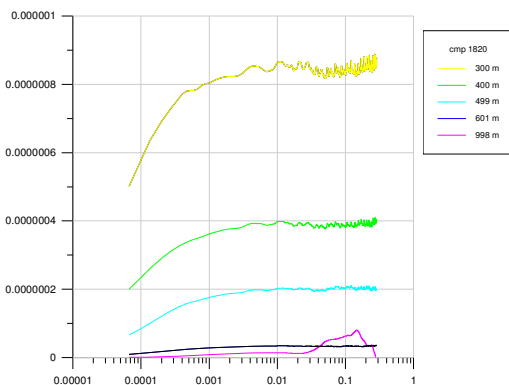


Figure 2. A step response for an offset of 200-300 m for Canada demonstration.

Experiments with synthetic data have shown that for a given target depth, offsets in the range 3 to 4 times target depth are most appropriate for inversion. Figure 1 shows that for each CMP position there are generally 3 or 4 offsets within that range and we can employ them all simultaneously to derive the best fitting layered model for that CMP.

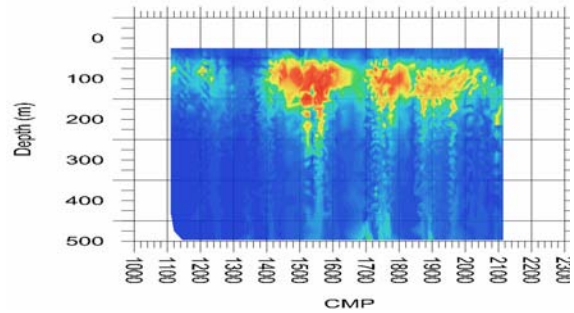


Figure 3. 1D inversion for Canada demonstration

Since the forward problem is non-linear with respect to resistivity, we use a conventional linearised Occam inversion scheme to iterate to a solution from a given starting model. The model is parameterised by $n+1$ resistivities, n referring to layers of equal thicknesses and 1 relating to the underlying halfspace.

Convergence is generally achieved in about 6 iterations and Figure 2 shows the 1D model obtained.

3D Inversion

For 3D forward inversion we have currently been using INTEM3D code by Gabor Hursan and Michael Zhdanov from Consortium for Electromagnetic Modeling and Inversion, University of Utah. INTEM3D is based on the integral equation (IE) method and was designed for frequency domain electromagnetic modeling of 3D geoelectrical structures embedded in horizontally layered Earth.

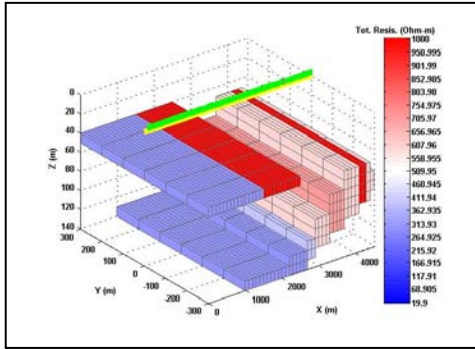


Figure 4. 3D model for Canada demonstration.

CONCLUSIONS

The MTEM method demonstrated its abilities for a high resistive target such as hydrocarbones in both on-land and marine application. Since MTEM genarates a varaty of frequencies that gives a signisacntly better resolution in comperison with any DC or controlled source soundings. 1D approach for inverting multi-offset MTEM data is illustrated with the ability to determine gross features of the subsurface resistivity variations both laterally and with depth. We expect it will provide a reliable starting model for more complex 3D inversion schemes which is under development.

REFERENCES

Wright, D., Ziolkowski, A., and Hobbs, B., 2002. Hydrocarbon detection and monitoring with a multichannel transient electromagnetic (MTEM) survey. The Leading Edge, 21, 852-864.

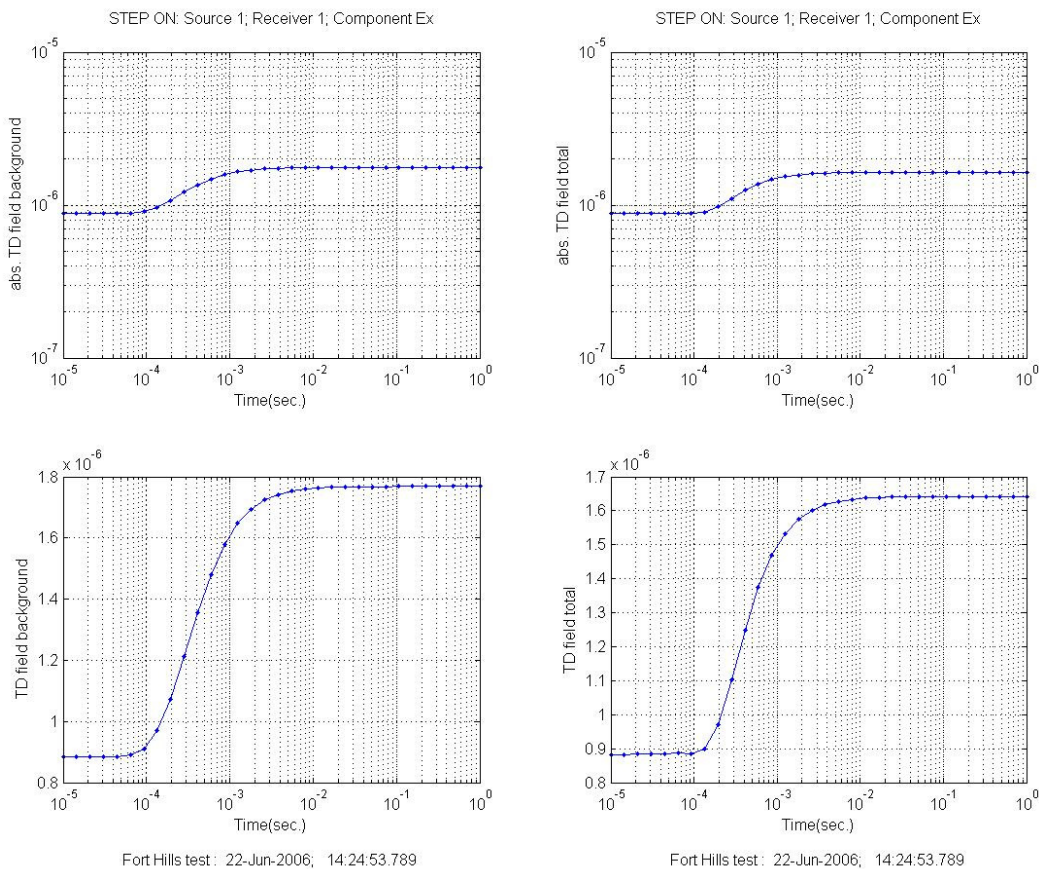


Figure 5. 3D forward response for the model shown at Figure 4.

Assessment and evaluation of groundwater using CSAMT method—an example from Beijing, Capital of China

Qingyun Di Ruo Wang and Guangjie Wang, Institute of Geology and Geophysics, Chinese Academy of Sciences.P.O.Box 9825, Beijing 10029, China.

SUMMARY

Geophysical exploration of groundwater in urban and suburban Beijing (Capital of China) suffers from a high-level ambient noise problem, which rises from cultural subsurface structures. This paper summarizes two successful applications of the controlled source audio-frequency magnetotelluric (CSAMT) method to groundwater exploration in Beijing area. The problem of the cultural noise was overcome by carefully selecting the output power, operating frequency, transmitter length, and receiver spacing.

The results, which were presented in the form of two-dimensional resistivity models, had shown a close agreement with the general hydrogeological condition of the area. Moreover the subsurface structure was clearly deduced from these results. Therefore, CSAMT method can give reasonably accurate results in areas with high level of cultural noise.

Keywords: CSAMT, groundwater, exploration, Beijing of China.

INTRODUCTION

The rapid socio-economic development in Beijing has increased the demand of water for all purposes. This has made the groundwater exploration an important target of the state government. The main water-bearing horizons in Beijing area are the sandstone and limestone aquifers. The geological information about these aquifers is limited due to their large depth of occurrence, and consequently their water is not as well exploited. The estimated depths are about several hundred meters. Such problem are amenable to surface geophysical prospecting.

Electrical and electromagnetic methods are the most popular of all the geophysical methods as far as groundwater exploration. However, the electrical methods suffer from the problem of the high level cultural noise, which are encountered in Beijing urban and suburban areas.

The CSAMT method was used due to its high signal-to-noise ratio (Piao, 1990; He, 1990; Fu, 1991; Misac, 1992; Fang, 1993; Bi, 2002). The CSAMT method was also used to detect deep subsurface structures (Wu et

al, 1996; He, 1990), which is particularly useful to investigate the deeply buried groundwater aquifers (Wu and Shi, 1996; Shi, 1999).

The present study was carried to test the possibilities and limitation of CSAMT surveys in the assessment and evaluation of groundwater as well as to delineate the subsurface geology and structure. Two examples were conducted in Beijing city during this work.

GEOLOGY HYDROGEOLOGICAL AND GEOELECTRICAL OF THE AREA

Beijing is located in the secondary tectonic element of North China (Bi, 2002). From Mesoproterozoic, the Beijing area has formed massive littoral facies deposit formation. Chang-cheng system, Ji-xian system and Qing-bai-kou system are distributed widely in the area. The deposition thickness is huge. There are many water-rich strata, such as carbonates and sandstone in Ji-xian system. There also are some water-rich strata in Cambrian and Ordovician. After the Cenozoic era, the northern China fault was formed in the Himalayas movement. As a section of the northwest China fault, a series of faulted-basins were formed in the Beijing area in Eogene, making some water-rich strata buried deeply.

The basis for the CSAMT method for ground exploration is the resistivity contrast between the water-bearing horizons and the surrounding dry rock units. The geoelectrical characteristics of the main rock units in the survey area have the following limits. The resistivity of the quaternary deposits is usually 10-100 Ω m. The resistivity of the sandstones generally ranges from 200 to 400 Ω m, while the resistivity of saturated sandstone varies from <30 to 90 Ω m. The resistivity of the volcanic rocks (Jurassic) is usually in the range of 1000-2000 Ω m. Usually the saturated fault zone has low resistivity compared with other strata. The drop in resistivity depends mainly on the water content and the porosity (including fractures and weathered zones).

CSAMT METHOD AND FIELD CONFIGURATION

The main task of the CSAMT survey is to delineate the depth of the saturated sandstone and limestone stratum, which represents the main groundwater reservoirs in Beijing area. As mentioned earlier, the survey area is characterized by high-level of cultural noise. To overcome this problem and to meet the main goals of this study, especial field configuration for CSAMT data acquisition was applied. Such configurations are to use a CSAMT system with an output power of 30kw. The electric dipole transmitter length reaches 2000m, and the distance between the source and receivers is up to 8km. The frequency is between 0.25Hz and 10000Hz. The receiver electrode spacing is usually 30-50m. Moreover a source current of 10 Ampere was only used, this can reduce the effect of the uppermost conductive layer, which is also encountered in Beijing area. The data acquisition mode is shown in Figure 1.

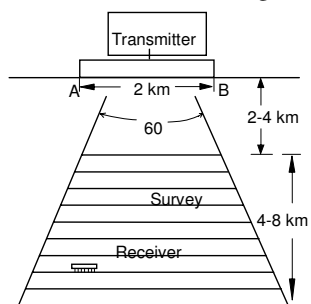


Figure 1. The sketch map of CSAMT data acquisition

Because the noise level in the Beijing urban area is several times higher than the mountain areas, the stack time of collecting the CSAMT data in this study is more than 10 minutes for each frequency (normally 3 minutes). Even so we still need to do the field noise and static corrections before data inversion.

The CSAMT surveys were started around Beijing area in the fall of 1994. So far, more than 20 groundwater

and geothermal exploration surveys have been done including the surveys carried out in the Yan-qing district of Beijing (Wu and Shi, 1996), Nan-yuan in Feng-tai district (Wu and Shi, 1996), and the Olympic park of Beijing (Xu, 2002; Liu, 2002).

THE RESULTS AND INTERPRETATION OF THE TWO FIELD EXAMPLES

The paper will introduce two examples of groundwater exploration results. These are the eighth water plant of Beijing water supplying base in Beijing suburban Niu-lan-shan and the Olympic park of Beijing.

Case 1 – The eighth water plant of Beijing water supplying base in Beijing suburb Niu-lan-shan. This water supplying plant represents one of the main drinking water resources that supplying Beijing people. The area located in the northern east part of Beijing city. It is about 30km far from Olympic park and close to the Da-hu-ying village.

In this area, a CSAMT line of 1100 meters was conducted in the northeast (10-degree) direction along the water supplying wells VII, VIII, IX, and X (Figure.3), the well VIII is almost at the center of the profile. Due to the Build area and roadblock the survey line was not extend to the wells VII and IX. The distance between the two transmitting electrodes is 1200 meters, and the distance between the transmitter and receiver is 4 Km, the spacing between receiver stations is 30 meters. The maximum transmitting current is 12A. The frequency series is 8192~16Hz. In order to eliminate the industrial power noises, a 50Hz notch filter was applied.

Figure 2 shows a CSAMT inversion section along the survey line. The inversion result clearly distinguished four resistivity zones. The upper zone represents the main water-bearing horizon, which is mainly consisting of sand and gravels. It has a thickness up to 100m. The resistivity value range from 70 to 120 Ω m, possibly suggest fresh water zone. The upper zone is underlain by low resistivity zone (20-30 Ω m) indicating saturated clay horizon with some sand lenses; it has a thickness of about 150m. The lower most part of the model shows a high resistivity values ranges from 120 to 350 Ω m due to crystalline volcanic rocks, which in turn overlain by low resistivity values (50 - 120 Ω m) possibly suggested saturated weathered zone.

The interpreted resistivity results presented in Figure 2 have clearly shown a good agreement and fit with the general geological and hydrogeological information in Figure 3.

Case 2 – The Olympic park of Beijing. The CSAMT measurements were also conducted in the Olympic

park to investigate the deep geothermal groundwater resources, which are possibly related to the Gao-li-ying fault. This fault was detected previously from the geology information and it is passing through the Olympic park area.

A CSAMT line of 800 meters was laid in a northeast (98-degree) direction. The distance between the two transmitting electrodes is 1300 meters, and the distance between the transmitter and receiver is 8 Km, the spacing between receiver stations is 10 meters. The maximum transmitting current is 16A. The frequency series is 8192~8Hz. In order to eliminate the industrial power noises, a 50Hz notch filter is used.

The interpreted resistivity model shown in Figure 4 is well identified the Gao-li-ying fault. The left side of the fault (foot wall) has a high resistivity value more than 150 Ωm due to the thick Conglomerate layer. The right side of the fault (hanging wall) has relatively low resistivity less than 90 Ωm possibly suggests saturated sandstone horizon. The resistivity in the upper part of the model varies from high to low resistivity due to the variation in lithology which is mainly consist of arenaceous clay of Quaternary age with some manmade buried material.

CONCLUSIONS

The CSAMT method has proven to be a powerful tool to work in a high-level cultural noise environment. The interpreted results of the CSAMT method had shown a close agreement with the general hydrogeological condition in the urban and suburban Beijing area. The results also reinforced the suitability of the CSAMT method in the assessment and evaluation of groundwater reservoirs. The method is also capable to delineate the subsurface structures, particularly in identifying fault zones filled with water.

ACKNOWLEDGEMENTS

Many thanks given to Professor Miaoyue Wang and Dr. Elzein for their good suggestions for the paper. We also thank the financial support from the project 40235055.

REFERENCES

- Bi, D. Z., Beijing geothermal resource. Beijing: Geological Publishing House, 2002.
- Fang, W.Z., Theory Of transient electromagnetic sounding survey. Northwestern Polytechnic University Press, 1993.
- Fu, L. K., The course in applied geophysics. Beijing: Geological Publishing Press. 1991.
- He, J. S., Controlled source audio magnetotelluric method. Changsha: Central South of Technology University Press, 1990.
- Misac, N. N., Electromagnetic methods in applied geophysics. Translated by Zhao Jing-Xiang, et al. Beijing: Geological Publishing House, 1992.
- Piao, H. R., Principle of Electromagnetic Sounding. Beijing: Geological Publishing, 1990.
- Shi, K. F., Theory and Application of CSAMT Method. Beijing: Science Press, 1999.
- Wu, L. P., Shi, K. F., 1996, Model discussion for geothermal exploration and formation Song-shan. Geophysical and Geochemical Prospecting.
- Wu, L. P., Shi, K.F., 1996, Applied study of CSAMT method on ground water exploration. Chinese Journal of Geophysics, 39, 712-717.

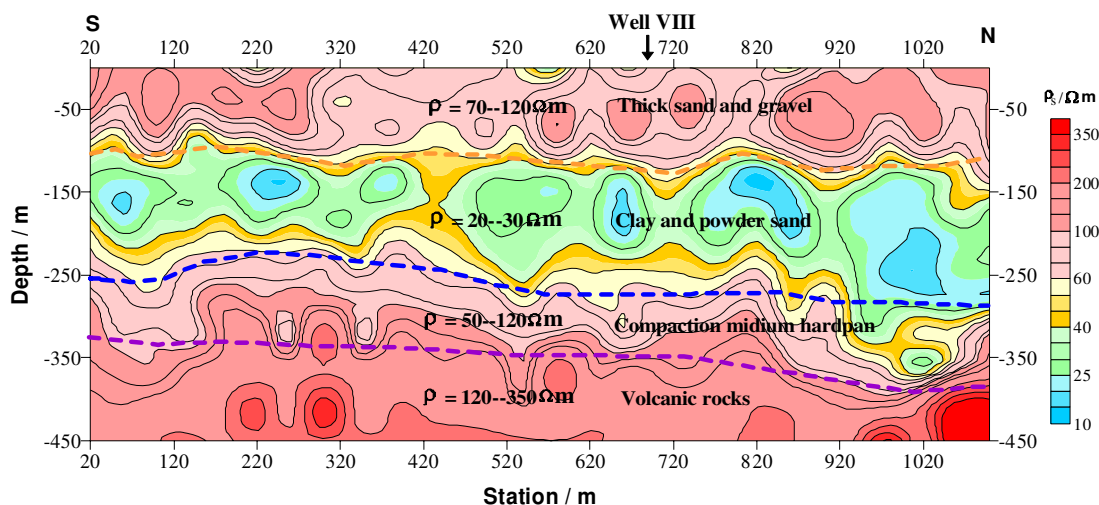


Figure 2. The CSAMT inversion result and interpretation for the eighth water plant

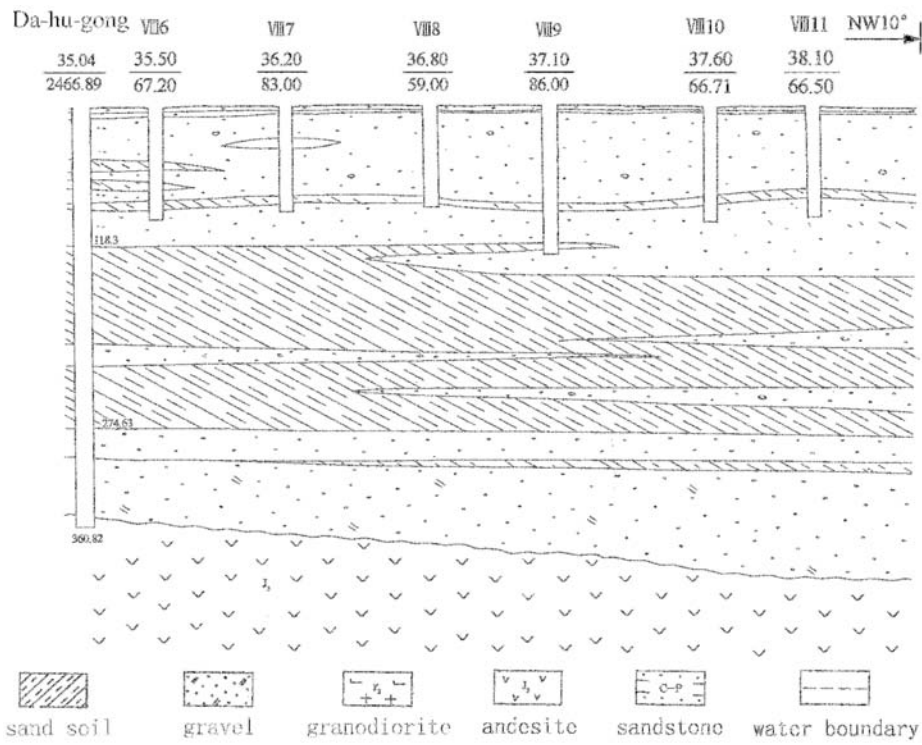


Figure 3. The geology section in the area of the eighth water plant

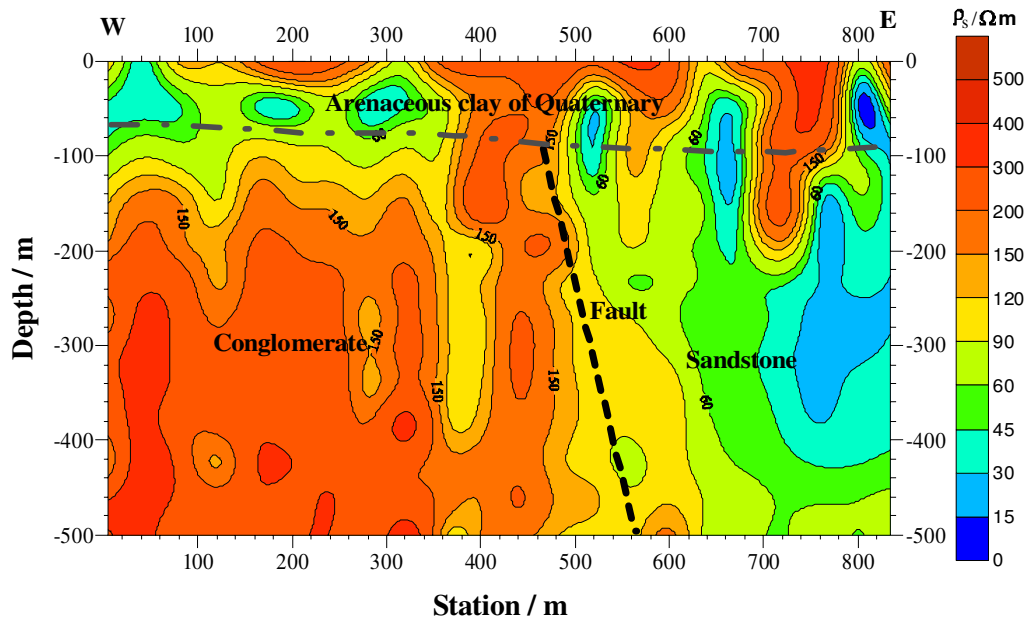


Figure 4. The CSAMT inversion result and geology interpretation for the Olympic park survey

Combined interpretation of DC resistivity and TEM soundings at Hammam Mousa hot spring, Sinai, Egypt

Gad El-Qady, National Research Institute of Astronomy and Geophysics, Helwan, Cairo, Egypt

Usama Saad, National Research Institute of Astronomy and Geophysics, Helwan, Cairo, Egypt

Fernando Santos, Centro de Geofisica da Universidade de Lisboa, Lisboa, Portugal

Sultan Awad and El-Said Ahmed, National Research Institute of Astronomy and Geophysics, Helwan, Cairo, Egypt

SUMMARY

Goelectrical methods are pioneer in geothermal exploration. With the advent of computing technology, it has become convenient to apply sophisticated data analysis and joint inversion to goelectrical field data. In this work, a goelectrical survey was conducted at the Hammam Mousa area, Sinai, Egypt, to explore the geothermal resources and groundwater aquifer. The field survey comprises 19 VES of DC resistivity with AB/2 up to 1000m and nine stations of Time Domain Electromagnetic (TEM) using square loop of side length of 25 m. Interpretation of 1-D inversion gave a layered-earth resistivity model using a nonlinear least-squares method for both data sets separately. However, due to the effect of both hot water and seawater seeped from the Gulf of Suez, the resistivity curves show low resistivity.

Numerous studies have shown that, the joint interpretation of galvanic and inductive data, where a single model satisfies both data sets, will generally enhance the resolution of the subsurface resistivity structure. Thus, the inclusion of inductive data in the VES data set must be expected to reduce problems with layer suppression, reduce the low resistivity equivalence, and drastically reduce the high resistivity equivalence otherwise encountered with this method. In this concern, the joint interpretation of both VES and TEM data, using the available geological information as a constraining factor, could successfully enhance the inversion results. The goelectric cross section resulted from the inversion process shows the effect of Gulf water intrusion in the western part of the study area. Meanwhile, hot water reduces the resistivity values drastically near to the hot spring.

Keywords: Dc resistivity, TEM soundings, Geothermal, Egypt.

INTRODUCTION

Geophysics, mainly goelectrical methods frequently are employed in exploration for geothermal resources. Goelectrical methods, in particular, have been employed in the study of most geothermal fields. Reviews as well as some characteristic examples are discussed by Thanassoulas (1991).

The Sinai Peninsula is considered as a bridge and barrier between the Asian and African Continents. Recently, new projects to settle the Bedouin have begun, and the development is transforming several coastal areas. Tectonically, the Sinai area is considered as an unstable shelf due to frequent earthquake activity and its geologic setting, which is controlled by tectonic activity at the Red Sea, Gulf of Suez, and Gulf of

Aqaba (Said, 1962). This tectonic activity has been accompanied by thermal activity represented by a cluster of thermal surface manifestations along the eastern shore of the Gulf of Suez. Among these thermal manifestations, Hammam Mousa (Moses's Bath) is representing one of the best known hot springs along the Gulf of Suez, located at El-Tor City, the capital of south Sinai (Fig. 1).

Consequently, the main goal of this study is to investigate the geothermal field and groundwater aquifer at Hammam Mousa hot spring using a joint goelectrical resistivity and TEM survey.

GEOLOGIC CONTEXT

Hammam Mousa area is located on the eastern shore of the Gulf of Suez (Fig. 1). The surface area near the hot

spring is composed of sabkha deposits. Far to the east, alluvial deposits dominate and occupy the surface of the El-Qaa plain. The subsurface geologic section is represented by Cretaceous (Campanian to Cenomanian) up to Miocene rocks (Said, 1962). During the Early Cretaceous, the study area was a shallow sea, and sandy sediments of the Nubian facies is represented. These sediments are overlain by Cenomanian beds, which are brownish and varicolored marls, with a clastic content of sand and shale (Kostandi, 1959, Said, 1961). Above the Cenomanian beds, the lower Turonian beds; represented by the Rudaeis Formation of soft marl and shale rest (Beadnell, 1927), the Lower Eocene beds of limestone with flint and marls of Thebes Formation rest unconformably above the Rudaeis Formation. This is followed by the laminated green and grey shale of Esna Formation of the Upper Paleocene (Said, 1962). At the top, the Quaternary clastic sediments of gravel, sand, clay and silt are represented by El-Tor Group. During the early Tertiary (Oligocene to Miocene), at the opening of the Red Sea Rift, some volcanic activities took place. In the western and central Sinai, there are many basaltic bodies mostly represented in the form of doleritic dikes, sills, plugs, and flows (Meneisy, 1990). Also, the great synclinal area of the El-Qaa Plain that lies to the east of the study area belongs to this episode of deformation. The major structural features are well defined NNW trending fault blocks, which tilt strongly eastward on their west side (Said, 1962).

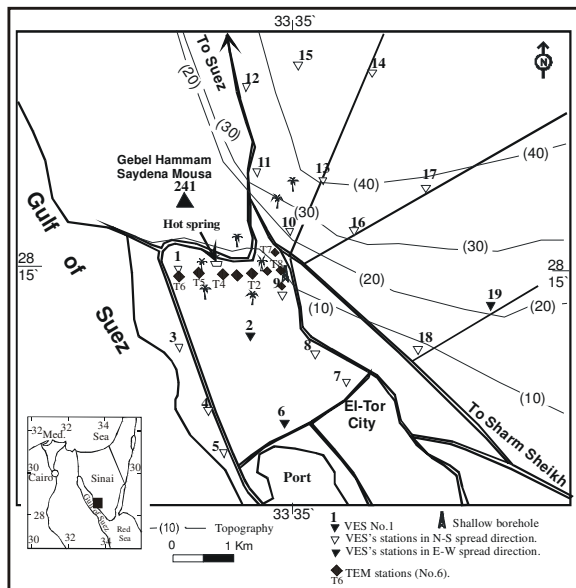


Figure 1. Location map for the study area and its surroundings showing VES stations (Topographic contours in meters).

GEOPHYSICAL EXPLORATION

The geophysical survey described in this work was carried out by DC resistivity and transient electromagnetic (TEM) soundings. The DC resistivity data was collected using a Schlumberger array. Nineteen VES stations were measured, (Fig. 1) using electrode spacing starting from $AB/2= 2$ up to 1000 m, in successive steps.

A reconnaissance electromagnetic survey comprises nine TEM stations were measured using Sirotem MK3, with single loop configuration, both 25 and 50 m loop side was used.

The apparent resistivity of DC soundings has relatively higher values in the shallow parts ($AB/2 = 4$ and 20 meters, respectively) compared to the deeper parts ($AB/2=1000$ m). Relatively low resistivity values characterize the central and southwestern parts of the study area. The resistivity field curves of all the stations have been inverted one dimensionally (Zohdy, 1989). Figure (2) shows an example of 1-D models and its correlation with the lithology of a nearby shallow log.

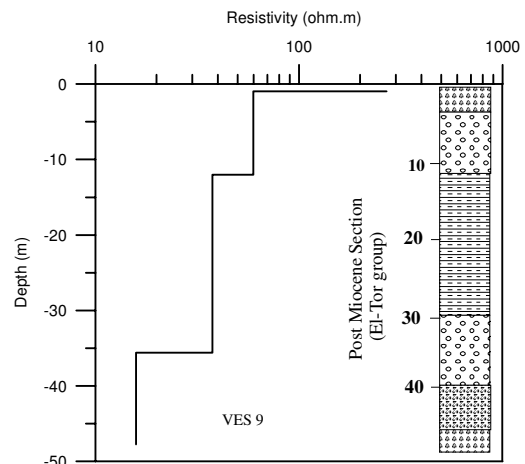


Figure 2. Correlation of Inverted 1-D model of VES 9 with the borehole information.

The TEM apparent resistivity data have been converted before modeling into effective subsurface resistivity at depth yielding a continuous picture of the resistivity-depth distribution of the subsurface. 1-D modeling was then used for forward and automatic inversion approaches of TEM data set (Temixxl, 2002).

Figure 3 shows the forward modeling at TEM station No.5. The initial model was selected at the nearest borehole, beside the site taking any guidance from Dc resistivity-depth transformation. As shown the fit between observed and calculated data is generally good.

Another example of 1-D inverse modeling results is given at site TEM station No.6 (Figs. 4). In these models, the thick conductive zone is clearly defined

and its boundaries are concordant with the alterations of resistivity-depth transformation which could be very useful for getting starting model if there is no a priori information. The distinction between the clay layer and the water bearing formation could be delineated. This is attributed to the high sensitivity of TEM method for detecting conductive zones.

CONCLUSIONS AND RECOMMENDATION

The present work aimed to delineate and elucidate the geothermal reservoir at Hammam Mousa Hot Spring.

To achieve this purpose a joint 1-D interpretation for Dc VES and TEM soundings had been conducted. It is clear that there is a huge thick, high conductive layer at depth ranging from 40 m up to 125 meters. That can be referred to the effect of geothermal water circulation or seawater intrusion in this part.

According to the interpretation of this data set, a promising area for geothermal drilling is recommended, around the hot spring and its neighborhood, where there is a considerable aquifer thickness. Although the 1-D interpretation has proved feasible and reliable in many practical cases, significant inaccuracies may occur when true geoelectrical structure is essentially multidimensional. In this case, multidimensional inversion scheme would be more useful. We hope future work will enable us to collect data set (3-D survey) for 3-D modeling scheme. In addition, a detailed geophysical survey is recommended using different geophysical resistivity tools, such as magnetotelluric and electromagnetic methods. These methods can overcome the problem of seawater intrusion and arid condition in this area.

REFERENCES

Beadnell, H. J., 1927, The wilderness of Sinai. Arnold, London, 180pp.

Kostandi A., 1959, Facies maps for the study of the Paleozoic and Mesozoic sedimentary basins of the Egyptian region. 1st Arab Petrol. Congr., Cairo 2: 44-62.

Meneisy M.Y., 1990, Volcanicity, Chapt.9, In Said, R.(Ed.) 1990. Geology of Egypt, Balkema Pub. Rotterdam, Netherlands, 157-172.

Said, R., 1961, Tectonic framework of Egypt and its influence on distribution of foraminifera. Bull.Am.Assoc.Petrol.Geol. 45: 198-218.

Said, R., 1962, The geology of Egypt. Elsevier, Amsterdam-New York, 377pp.

Sturchio, N, Arehart, G, Sultan, M. Sano, Y., Abokamar, Y. And Sayed M., 1996, Composition and origin of thermal waters in the Gulf of Suez area, Egypt. Applied Geochemistry, 11, 471-479.

TEMIX XL 4 2002, Temixxl v.4 user's manual. Interpex, 468 p

Thanassoulas C., 1991, Geothermal exploration using electrical methods. Geoexploration, 27, 312-350.

Zohdy, A., 1989, A new method for the automatic interpretation of Schlumberger and Wenner Sounding curves. Geophysics Vol.54 No.2, 245-253.

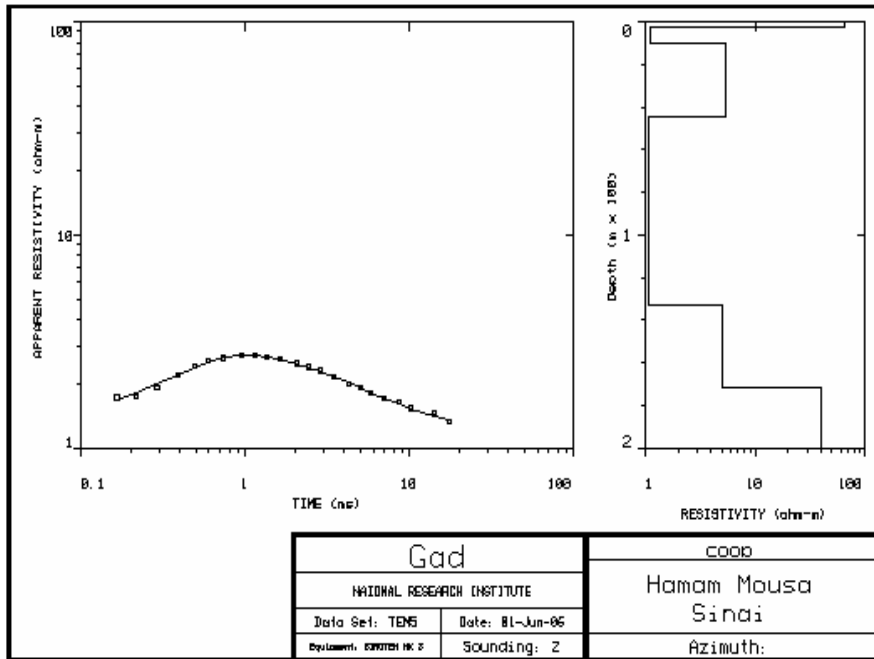


Figure 3. Interpretation of TEM station No. 5.

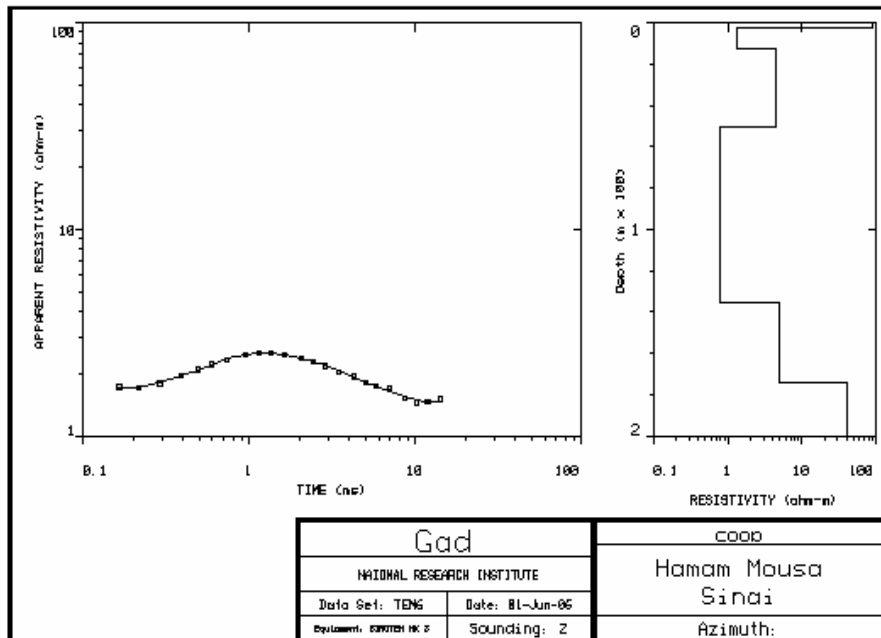


Figure 4. Interpretation of TEM station No. 6

3D modelling of magnetotelluric phase tensor data from the Rotokawa geothermal field, Taupo Volcanic Zone, New Zealand

Wiebke Heise, T. Grant Caldwell, Hugh M. Bibby
 GNS Science, Lower Hutt, New Zealand

SUMMARY

A 3D conductivity model of the high temperature geothermal system from New Zealand's Taupo Volcanic Zone has been constructed by iterative forward modelling of phase tensor data from a detailed 64 site magnetotelluric (MT) survey. An unexpected and interesting feature of this model is the presence of a surprisingly resistive ($>300\Omega\text{m}$) feature within the otherwise conductive material of the geothermal system. This feature appears to coincide with the high temperature ($>300^\circ$) core of the geothermal system.

Keywords: magnetotellurics, geothermal system, phase-tensor, 3D modelling

INTRODUCTION

The Taupo Volcanic Zone (TVZ), located in the North Island of New Zealand, is a region of recent rhyolitic volcanism and rapid crustal extension. This region is also characterised by exceptionally high heat flow, 4200 MW, which is discharged through 23 high temperature ($>250^\circ$) geothermal systems, Figure 1 (Bibby et al. 1995). The geothermal systems in the TVZ are marked by areas of low resistivity with a large resistivity contrast with the surrounding areas as can be seen in Figure 1.

The near surface low resistivities inside the geothermal fields are caused by the combination of high temperature, saline fluid and hydrothermal alteration of the young volcanics. At depths greater than ~ 500 m, the resistivity values to increase due to decreasing pore space and a change in the type of hydrothermal alteration products (clays) at higher temperatures.

The uppermost 1 – 2 km of the TVZ are composed of a mixture of rhyolite lavas, welded and unwelded ignimbrites and volcanoclastic sediment. This material is resistive ($\geq 300\Omega\text{m}$) at shallow depth except where it has been hydrothermally altered. However, at deeper levels, this same material becomes conductive ($10 - 30\Omega\text{m}$) at low temperatures due to a diagenetic aging process in which small amounts of conductive clays and zeolites are formed within the rhyolitic volcanics. Thus, outside the geothermal systems, the conductivity depth structure of the TVZ is characterised by a layer more conductive older volcanics. Beneath the 2 – 4 km

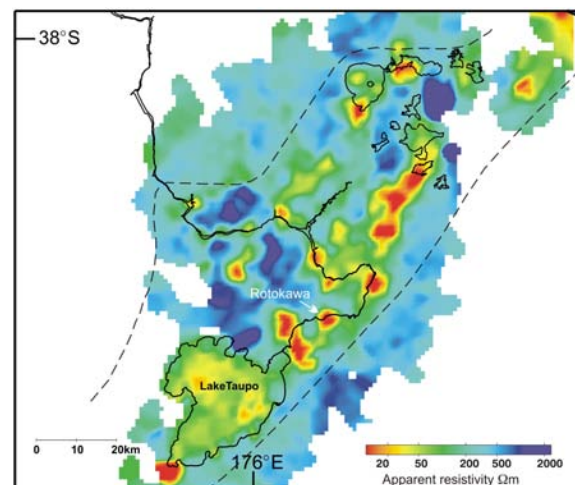


Figure 1. DC apparent resistivity map from Schlumberger array measurements made with an electrode spacing of (AB/2) 500 m. Conductive areas shown in red ($<30\Omega\text{m}$) mark the geothermal systems (Bibby et al., 1995).

of volcanics, the basement rocks (greywacke) are resistive (300 - 1500 Ωm).

MAGNETOTELLURIC DATA

Recently a broadband (3 ms – 2000 s) MT survey consisting of 64 sites was conducted to investigate the deeper structure of the Rotokawa geothermal field. Measurement sites have an average spacing of 200 m -

500 m in the central part of the geothermal field, i.e. the area characterised by the low resistivity anomaly (Figure 1).

3D MODELLING

3D forward modelling was carried out using the finite difference algorithm of Mackie and Booker (1999) as implemented in WinGLink. Detailed information about the near surface resistivities is provided by the DC resistivity mapping (Figure 1). The NE striking regional conductivity structure is known from long offset resistivity studies (Bibby et al. 1998; Risk, 2000) and regional MT studies (Ogawa et al., 1999) and reflects the down faulting of the greywacke basement along the margins of the TVZ.

This information along with knowledge of the local geology, provided by drill holes and other geophysical methods enabled the construction of an initial 3D resistivity model. The model was then refined by trial and error fitting of the phase tensor ellipses (Caldwell et al., 2004). This approach to the forward modelling ensures that the 3D nature of the dataset is honoured while avoiding any galvanic distortion of the data. Examples of the observed and calculated phase tensor ellipses are shown in Figure 2.

RESULTS AND DISCUSSION

Figure 3 shows an E-W cross-section of the 3D model. As expected, at shallow depth (15 m - 200 m) the geothermal field is characterised by low resistivities (2 - 5 Ωm) which increase with depth to $\sim 30 \Omega\text{m}$. Outside the geothermal system the top 500 m of young volcanics, are resistive (300 Ωm) but become more conductive (30 -10 Ωm) below about 600 m. An unexpected feature of the modelling was the requirement for a resistive body (500 Ωm) in the central part of the geothermal field at depths between 900 m and 2500 m.

Sensitivity tests indicate a body with resistivity of at least 300 Ωm and of limited extent is necessary to fit the low phases observed at periods between 0.2 s and 1s.

Assessing the overall degree of fit of the phase tensor data is difficult. In an attempt to do this we have calculated misfit tensors given by

$$\Delta = \mathbf{I} - (\Phi_{\text{obs}}^{-1} \Phi_{\text{mod}} + \Phi_{\text{mod}} \Phi_{\text{obs}}^{-1})/2,$$

where \mathbf{I} is the identity matrix. These are plotted in Figure 4 at each site for the same two periods as in Figure 2. Note that the misfit tensor ellipses have not been normalised. Thus, the magnitude of the misfit is indicated by the size of the ellipse and also by the colour we have used to fill the ellipses which is

determined by the value of $|\det \Delta|^{1/2}$. The ellipse orientation indicates the direction in which the maximum difference occurs. If the orientation of the misfit tensor ellipses are spatially coherent then a systematic mismatch of the conductivity structure is implied e.g. an incorrect orientation of the conductivity structure. No clear pattern of the misfit tensor major axes can be seen in Figure 4. This suggests the model has captured the main features of the data.

CONCLUSIONS

The most exciting and notable feature of the modelling is the requirement for a high resistivity body in the central part of the geothermal field. This feature cannot be correlated with the geology known from drill holes, but correlates spatially with the area of highest temperature. Thus it appears we are imaging the resistive high temperature ($>300^\circ$) core of the geothermal system.

ACKNOWLEDGEMENTS

We thank Mighty River Power for kindly providing the MT dataset.

REFERENCES

- Bibby, H.M., Caldwell, T.G., Davey, F.J. and Webb, T.H., 1995. Geophysical evidence on the structure of the Taupo Volcanic Zone and its hydrothermal circulation. *Journal of Volcanology and Geothermal Research*, 68, 29-58.
- Bibby, H.M., Caldwell and Risk, G.F., 1998. Electrical resistivity image of the upper crust within the Taupo Volcanic Zone, New Zealand. *Journal of Geophysical Research*, 103, 9665-9680.
- Caldwell, T.G., Bibby, H.M. and Brown, C., 2004. The magnetotelluric phase tensor. *Geophysical Journal International*, 158, 457-469.
- Mackie, R.L. and Booker, J., 1999. Documentation for mtd3fwd and d3-to-mt. GSY-USA, Inc., 2261 Market St., Suite 643, San Francisco, CA 94114. User documentation.
- Ogawa, Y., Bibby, H.M., Caldwell, T.G., Takakura, S., Matsushima, N., Bennie, S.L., Tosha, T. and Nishi, Y., 1999. Wide-band magnetotelluric measurements across the Taupo volcanic zone: preliminary results. *Geophysical Research Letters*, 26, 3673-3676.
- Risk, G.F., 2000. Electrical resistivity surveys of the Rotokawa geothermal field, New Zealand. p. 121-126 In: Dunstall, M.G.; Morgan, O.E.; Simmons, S.F. (eds.) *Proceedings of the 22nd New Zealand Geothermal Workshop 2000*. Auckland: University of Auckland.

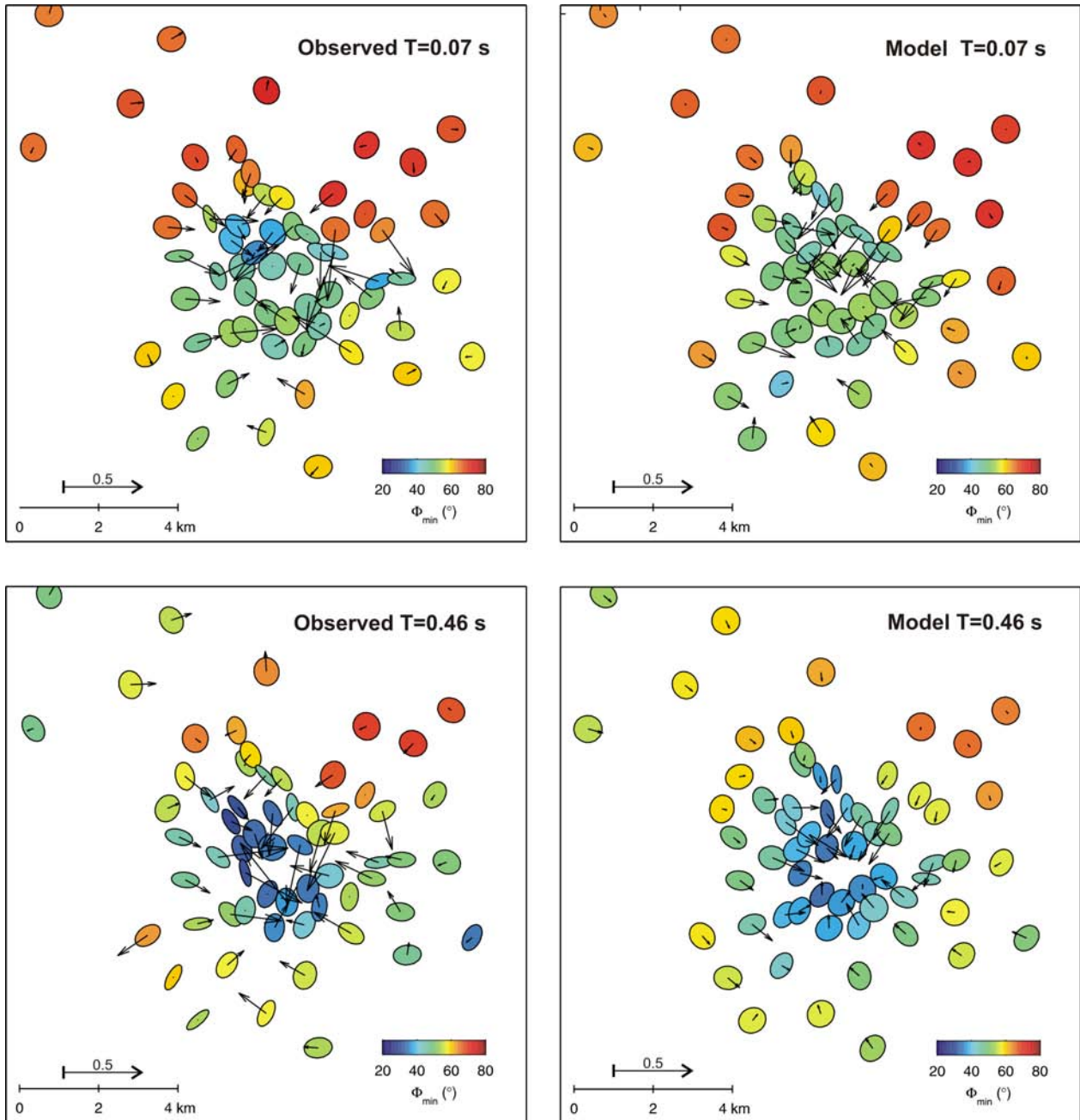


Figure 2. Phase tensor ellipses and real induction arrows (reversed, Parkinson convention) at 0.07 s and 0.46 s. Left panels show the data, right panels the response from the 3D model. The ellipses are normalised with Φ_{\max} and the colour scale shows Φ_{\min} . The high values of Φ_{\min} outside the geothermal system indicate decreasing resistivity, caused by the conductive volcaniclastics. Note the low phase values in the centre of the geothermal system for 0.46 s indicating a resistor at depth. Induction arrows are dominated by the strong conductivity contrast at shallow depths.

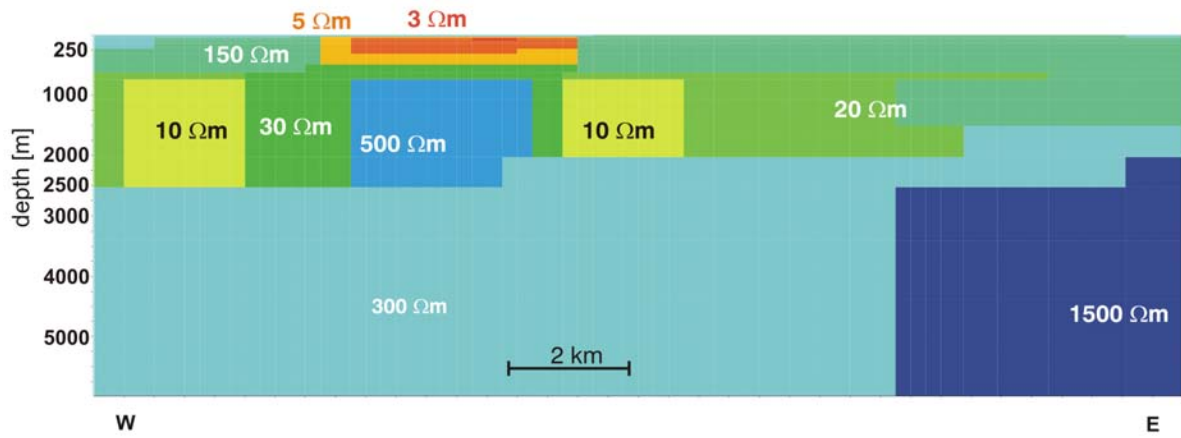


Figure 3. West-East cross section of the 3D forward model through the centre of the geothermal system.

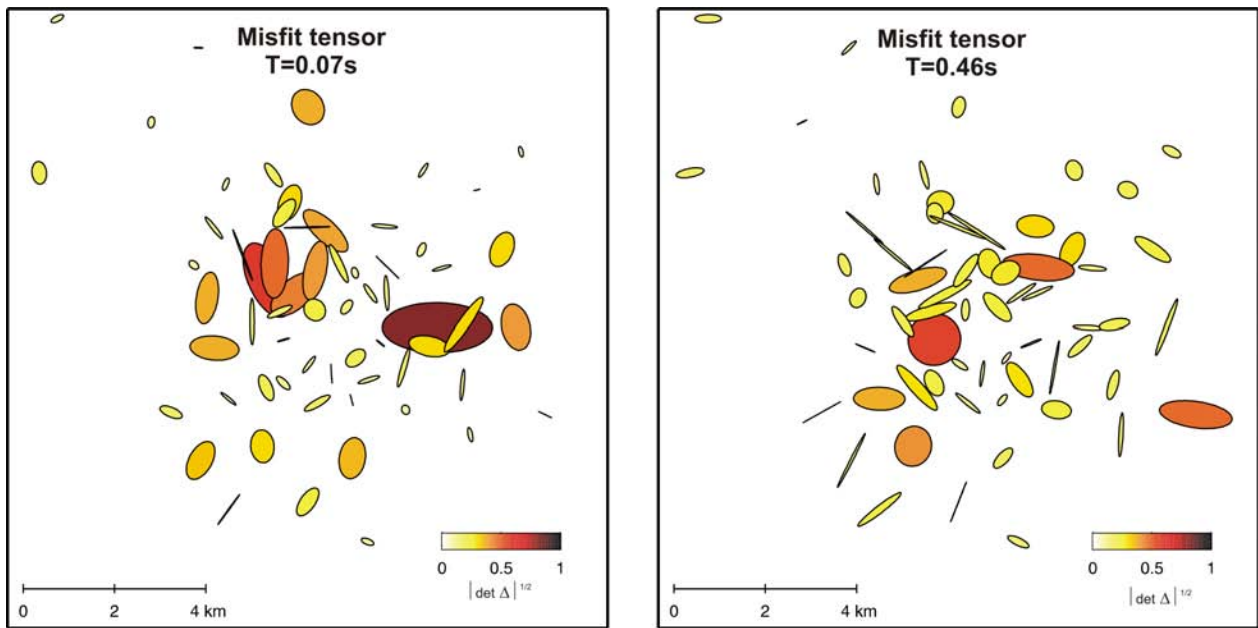


Figure 4. Phase tensor misfit at 0.07s and 0.46s. The colour fill of the ellipses shows $|\det \Delta|^{1/2}$ with $\Delta = \mathbf{I} - (\Phi_{\text{obs}}^{-1} \Phi_{\text{mod}} + \Phi_{\text{mod}} \Phi_{\text{obs}}^{-1})/2$.

Preliminary Magnetotelluric survey results of Arus-Bogoria geothermal prospect, Kenya

Josphat Mulwa, University of Nairobi, Department of Geology, P.O. Box 30197, Nairobi, Kenya
Nicholas Mariita, Kenya Electricity Generating Co. Ltd., Olkaria Geothermal Project, P.O. Box 785, Naivasha, Kenya

Justus Barongo, University of Nairobi, Department of Geology, P.O. Box 30197, Nairobi, Kenya
Jayanti Patel, University of Nairobi, Department of Physics, P.O. Box 30197, Nairobi, Kenya

SUMMARY

Arus-Bogoria geothermal prospect is located in Baringo-Bogoria basin, about 250 km from the city of Nairobi on the floor of Kenya Rift Valley (KRV). It is bound by latitudes 0° and 0.5° N and longitudes 35.87° and 36.17° E. Geothermal surface manifestations include hot springs and spouting geysers on the shores of L. Bogoria, fumaroles/steam jets at Arus and mud pools which extend for several hundred meters on the east bank of Molo river. The prospect area is overlain by Miocene-Pliocene lavas mainly trachytes, trachyphonolites and basalts. The terrain is characterized by extensive faulting and this forms numerous N-S ridges and fault scarps.

In this extended abstract, we discuss preliminary magnetotelluric (MT) survey results of Arus-Bogoria geothermal prospect in Kenya. In order to evaluate the potential of the prospect for generation of geothermal power, a total of about 40 MT soundings were conducted between March-July 2005 using Phoenix V5 MT system. The MT data were recorded in frequencies of 340 Hz to 0.001Hz using a coherency factor of 0.85.

The preliminary MT survey results at sea-level (~1300 m below ground level) show a NW-SE trending low resistivity (2-10 Ω -m) anomaly through L. Bogoria and relatively high resistivity (20-35 Ω -m) anomaly that trends in a N-S and NE-SW directions. The low resistivity anomaly is most likely due to the influence of Bogoria-Emsos-Legisianana fault (trending NW-SE to the east of L. Bogoria) which is channeling hot geothermal fluids. At deeper levels, the NE-SW trending high resistivity anomaly is prominent and it intersects the low resistivity anomaly.

Detailed MT and gravity surveys need to be undertaken in order to characterize the nature of the subsurface, geothermal resource and determine the geothermal resource potential of Arus-Bogoria geothermal prospect.

Keywords: Arus-Bogoria, geothermal, magnetotelluric survey, resistivity anomaly.

INTRODUCTION

Kenya is dissected longitudinally by the East African Rift System (EARS), here in referred to as the Kenya Rift Valley (KRV) where medium to high temperature (>140°C) geothermal fields are located (Figure 1). These geothermal fields are associated with Quaternary volcanic centers and fissures related to the rift floor fault systems (Riaroh and Okoth 1994; Omenda 2001). Only a few of these geothermal fields have been explored in detail for the purpose of determining their potential for generation of geothermal power. Olkaria

geothermal field is currently being exploited for generation of geothermal power with current output standing at about 127 MW_e which is approximately 13% of the national electric consumption.

Kenya has an extensive geothermal resource potential of more than 2000 MW_e that can be generated using conventional steam condensing turbines. These generation may exceed 3000 MW_e when combined cycle and binary systems are used (Omenda 2001). Hence, exploration for geothermal resources has been intensified along the Kenya Rift Valley.

In this extended abstract, we present some preliminary results of MT survey undertaken in Arus-Bogoria geothermal prospect as part of the geothermal resource exploration programme in Kenya.

Arus-Bogoria geothermal prospect is located in Baringo-Bogoria basin, about 250 km from the city of Nairobi and on the floor of central Kenya Rift Valley (KRV). It is bound by latitudes 0° and 0.5° N and longitudes 35.87° and 36.17° E (Figures 1 and 2). Geothermal surface manifestations include hot springs and spouting geysers on the shores of L. Bogoria, fumaroles/steam jets at Arus (Figure 2) and mud pools which extend for several hundred meters on the east bank of Molo river. The prospect area is overlain by Miocene-Pliocene lavas mainly trachytes, trachyphonolites and basalts (Baker and Wohlenberg 1971; Smith and Mosley 1993).

Extensive faulting accompanied by block tilting characterize the terrain and these form numerous N-S ridges and fault scarps. According to Baker and Wohlenberg (1971) this complex network of faults and fractures suggests reactivation of tensional strain oblique to the primary rift axis.

PREVIOUS WORK

Generally, the central Kenya rift valley and particularly the Arus-Bogoria area has been the target of a number of recent geophysical and geological investigations (Prodehl et al. 1994,1997; Simiyu and Keller 1997, 2001; Mariita 2003). These investigations have focused attention on the seismicity, velocity, crustal and mantle structures of the Kenya Rift Valley but not on the assessment of the geothermal potential of Arus-Bogoria area.

Regional gravity analysis by Simiyu and Keller (2001) and Mariita (2003) indicate no existence of volcanic heat sources in Arus-Bogoria area. Gravity analysis by Simiyu and Keller (2001) along an axial rift profile show a series of positive gravity highs at Menengai, Eburru, Olkaria and Suswa geothermal fields (Figure 1). The gravity highs have been modeled as resulting from volcanic centers underlain by discrete mafic bodies having a density of $2.9 \times 10^3 \text{ kg m}^{-3}$ which are presumed to be the heat sources for these geothermal fields. Cross-rift gravity profile by Mariita (2003) at latitude 0.6° N just to the north of Arus-Bogoria geothermal prospect shows that this area is underlain by about 2-4 km thick low density ($2.3 \times 10^3 \text{ kg m}^{-3}$) Miocene lavas and sediments but no evidence of volcanic intrusives which could be possible heat sources.

Young et al. (1991); Tongue (1992); Tongue et al. (1992, 1994) and have identified the Arus-Bogoria area

as an area of relatively high seismic activity in comparison to other geothermal areas along the KRV.

Recent geochemical work (Karingithi 2006) indicates that a geothermal resource exists in Arus-Bogoria. The reservoir temperature ranges between 115 to 425°C and the upflow zone may be located in the area close to the arus steam jets (Figure 2).

METHOD

Magnetotelluric (MT) survey technique (Cagniard 1953; Vozoff 1992) was used in an attempt to delineate and map the extent of possible geothermal resource in Arus-Bogoria area. The MT sounding surveys were carried out in 43 field stations between March-July 2005 using the standard MT measurement method involving two electric and three magnetic channels. The electric channels were aligned in north-south and east-west directions with 70 m of separation between the electrodes and consisted of lead-lead chloride porous pot electrodes. The magnetic field variations in north-south, east-west and vertical directions were measured using induction coil magnetometers equipped with MTC-50 coils. The measuring equipment consisted of MTU V5 system 2000 manufactured by Phoenix Geophysics Limited of Canada. The MT data was acquired in the frequency range of 340 Hz to 0.001Hz and the coherency factor was set at 0.85. Fast Fourier transforms and cascade decimation techniques were used to determine the auto- and cross-power spectra required for computing the frequency variation of the apparent resistivity and phase (Wight and Bostic 1980).

DISCUSSION OF MT SURVEY RESULTS

One dimensional inverse modeling was employed in the interpretation of transverse electric (TE) mode of the MT data after correcting for static shift using Transient Electromagnetic (TEM) data undertaken simultaneously.

The preliminary MT survey interpretation results at sea-level (~ 1300 m below ground level) show a NW-SE trending low resistivity (2-10 $\Omega\text{-m}$) anomaly through L. Bogoria (Figure 3). The low resistivity anomaly coincides with the location of Bogoria-Emsos-Legisianana fault trending in a northwest-southeast direction to the east of L. Bogoria as shown in Figure 2. The low resistivity anomaly intersects a relatively high resistivity ($> 10 \Omega\text{-m}$) anomaly that trends in a north-south and northeast-southwest directions. At deeper levels, this high resistivity anomaly is more prominent and continuous in north-south and northeast-southwest directions (Figures 4, 5, 6 and 7).

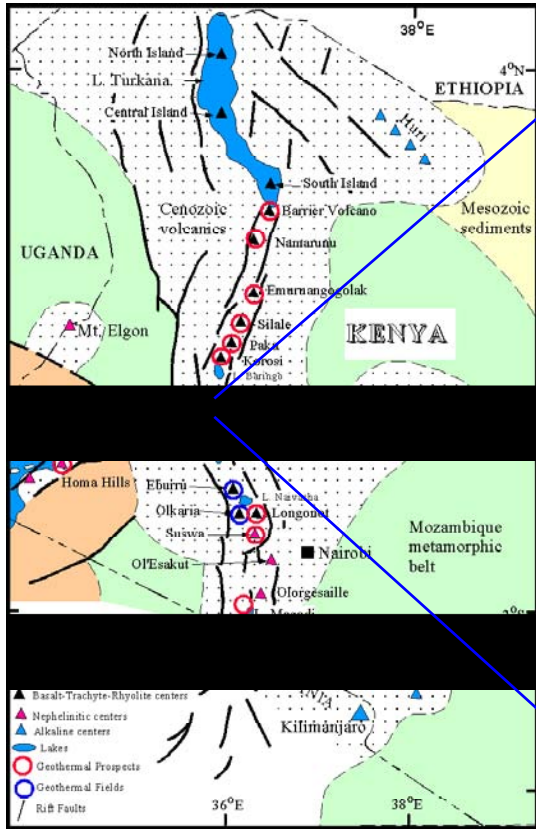


Figure 1. Location of Arus-Bogoria geothermal prospect in the Kenya Rift Valley

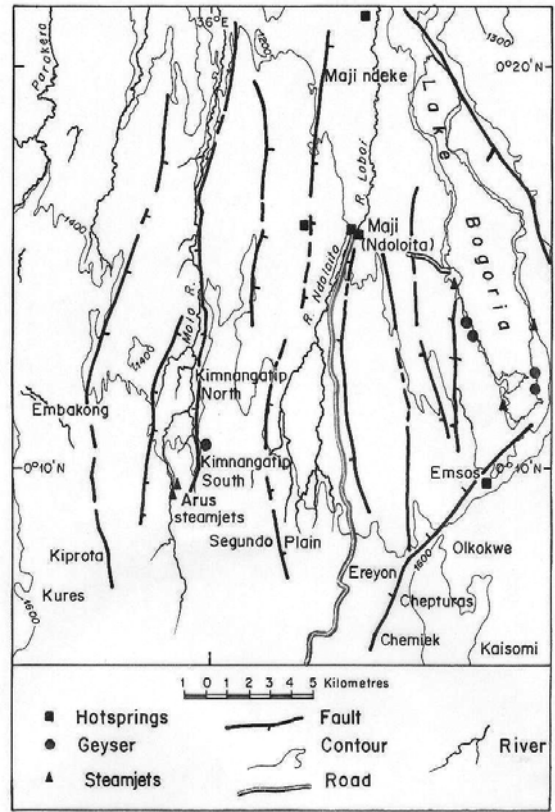


Figure 2. Structures and geothermal manifestations of Arus-Bogoria geothermal prospect

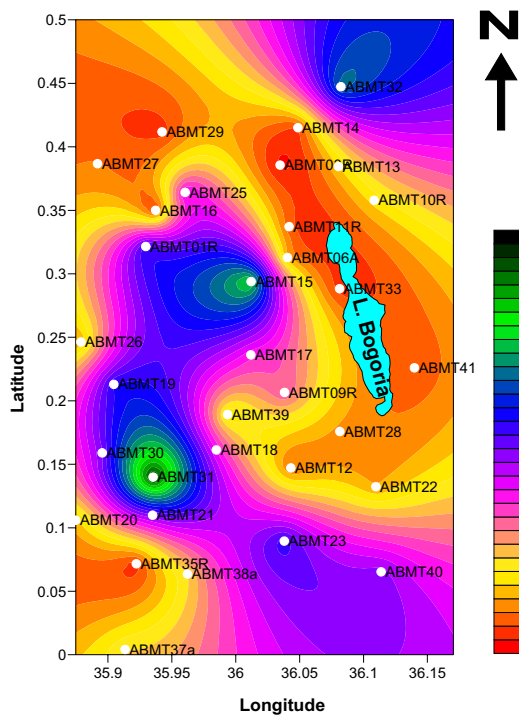


Figure 3. Resistivity distribution at sea-level

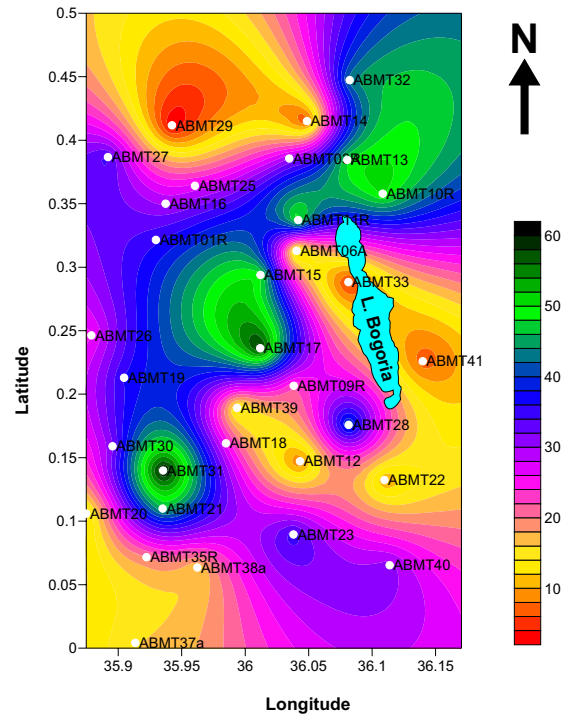


Figure 4. Resistivity distribution at 1000 m below sea-level

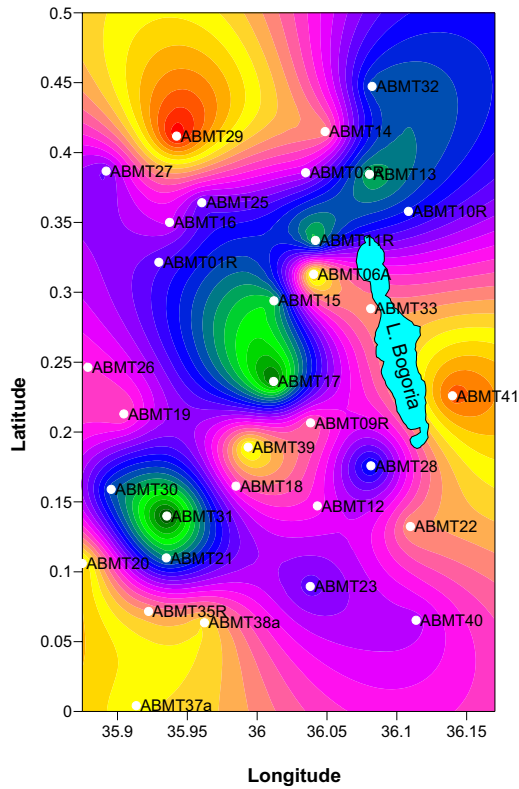


Figure 5. Resistivity distribution at 2000 m below sea-level

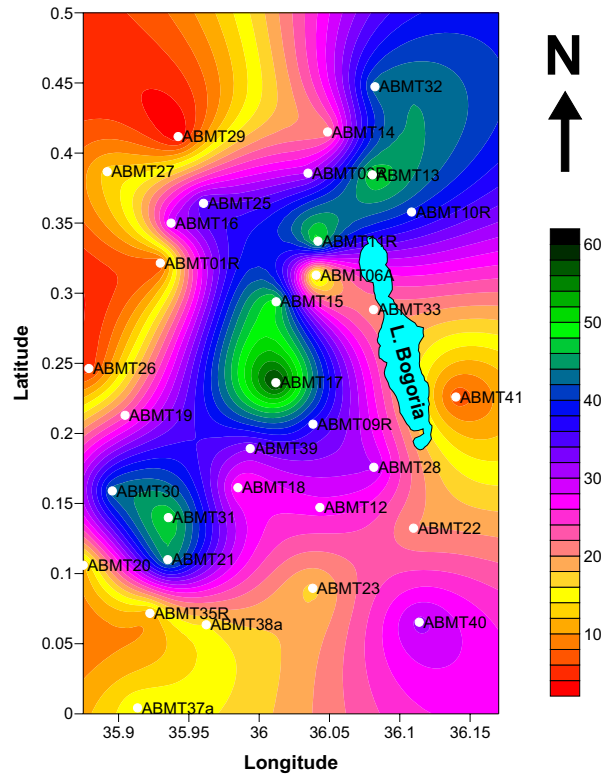


Figure 7. Resistivity distribution at 5000 m below sea-level

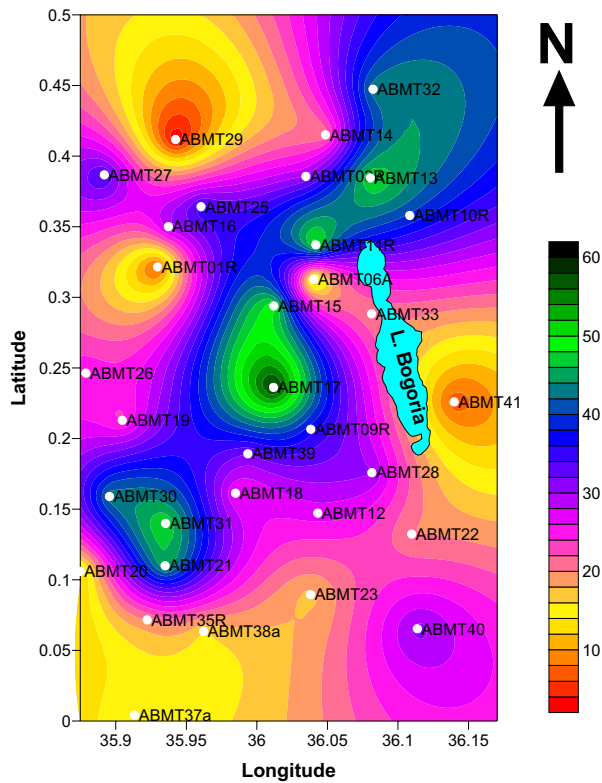


Figure 6. Resistivity distribution at 3000 m below sea-level

CONCLUSION AND FURTHER WORK

A low resistivity anomaly is evident in Arus-Bogoria geothermal prospect. This anomaly is related to Bogoria-Emsos-Legisianana fault which trends in a NW-SE direction on the eastern margin of Lake Bogoria. The fault is probably channeling geothermal fluids from an upflow zone.

Recent geochemical work indicates that a geothermal resource exists in Arus-Bogoria and the upflow zone is located close to arus steam jets. However, this upflow zone is not evident from the current MT survey.

Although previous gravity and the current MT data analysis shows no evidence of a heat source in Arus-Bogoria, the gravity data used in previous studies is too sparse to give a detailed picture of localized anomalies. There is need therefore for detailed MT and gravity survey in order to determine the nature of the subsurface and the source of geothermal manifestations.

The detailed survey will be able to elucidate whether Arus-Bogoria geothermal prospect is a geothermal system due to the “thermal blanket model” or whether it is a discharge point of geothermal fluids from Baringo/Korosi and Menengai geothermal prospects in

the north and south respectively due to its location in a topographic low.

ACKNOWLEDGEMENTS

The principal author would like to thank Kenya Electricity Generating Company (K) Ltd. for allowing him to participate in the MT field survey as part of his higher degree studies. He is also indebted to Dr. Mariita for accepting to supervise this study. Phoenix Geophysics Ltd. has granted the principal author a three year academic license to use Phoenix Geophysics softwares for data processing and is highly acknowledged.

REFERENCES

- Baker, B.H. and Wohlenberg, J., 1971. Structure and evolution of the Kenya rift valley. *Nature*, 229, 538-542.
- Cagniard, L., 1953. Basic theory of the magnetotelluric method of geophysical prospecting. *Geophysics*, 18, 605-635.
- Karingithi, C., 2006. The geochemistry of Arus and Bogoria geothermal prospects. 11th conference of the Geological Society of Kenya. *Geology for Industrial Growth, Wealth Creation and Poverty alleviation*.
- Mariita, N.O., 2003. An Integrated geophysical study of the northern Kenya rift crustal structure: Implications for geothermal energy prospecting for Menengai area. PhD dissertation, University of Texas at El Paso, USA.
- Omenda, P.A., 2001. An update on the status of geothermal resource exploration and development in Kenya. In: *Proceedings on commercial development of geothermal power projects in Kenya*.
- Phoenix Geophysics Ltd., 2003. *Data Processing User Guide: SSMT2000, SyncTSV and MTEdit, Version 2*, July 2003. Victoria Park, Toronto, Canada.
- Phoenix Geophysics Ltd., 2004. *V5 System 2000 MTU/MTU-A user guide, Version 1.4*, July 2004. Victoria Park, Toronto, Canada.
- Prodehl, C., Keller, G.R. and Khan, M.A., (Eds), 1994. Crustal and Upper mantle structure of the Kenya Rift. *Tectonophysics*, 236, 2-483.
- Prodehl, C., Ritter, J., Mechie, J., Keller, G.R., Khan, M.A., Fuchs, K., Nyambok, I.O. and Obel, J.D., 1997. The KRISP 94 Lithospheric investigation of southern Kenya-the experiments and their main results. In: *Stress and stress release in the Lithosphere*. Edited by Fuchs, K., Altherr, R., Muller, B. and Prodehl, C., *Tectonophysics*, 278, 121-148.
- Riaroh, D. and Okoth, W., 1994. The geothermal fields of the Kenya rift. *Tectonophysics*, 236, 117-130.
- Simiyu, S.M. and Keller, G.R., 1997. Integrated geophysical analysis of the East African Plateau from gravity and recent seismic studies. In: *Stress and stress release in the Lithosphere*. Edited by Fuchs, K., Altherr, R., Müller, B. and Prodehl, C., *Tectonophysics*, 278, 291-314.
- Simiyu, S.M. and Keller, G.R., 2001. An integrated geophysical analysis of the upper crust of the southern Kenya rift. *Geophys. J. Int.*, 147, 543-561.
- Smith, M. and Mosley, P.N., 1993. Crustal heterogeneity and basement influence on the development of the Kenya Rift, East Africa. *Tectonics* 12, 591-606.
- Tongue, J.A., 1992. Tomographic study of local earthquake data from the Lake Bogoria region of the Kenya Rift Valley. *Geophys. J. Int.*, 109, 249-258.
- Tongue, J., Maguire, P. and Burton, P., 1994. An earthquake study in the Lake Baringo basin of the central Kenya Rift. *Tectonophysics*, 236, 151-164.
- Tongue, J.A., Maguire, P.K.H. and Young, P.A.V., 1992. Seismicity distribution from temporary earthquake recording networks in Kenya. *Tectonophysics*, 204, 71-79.
- Vozoff, K., 1992. The magnetotelluric method. In: Nabighian, M.N. (Ed.), *Electromagnetic methods in applied geophysics*, Vol. 2. SEG, pp. 641-712.
- Wight, D.E. and Bostic, F.X., 1980. Cascade decimation-a technique for real time estimation of power spectra. *Proc. IEEE Int. Conf. Acoustic, Speech and Signal Processing*. Denver, Co., 626-629.
- Young, P.A.V., Maguire, P.K.H., Laffoley, N.d'A. and Evans, J.R., 1991. Implications of the distribution of seismicity near Lake Bogoria in the Kenya Rift. *Geophys. J. Int.*, 105, 665-674.

Possible magmatic input to the Dixie Valley geothermal field, Nevada, USA, with implications for district-scale resource exploration, inferred from MT surveying

Philip E. Wannamaker, University of Utah, Energy & Geoscience Institute, Salt Lake City, Utah, U.S.A.
Derrick P. Hasterok, University of Utah, Department of Geology and Geophysics, Salt Lake City, U.S.A.
William M. Doerner, Quantec Geoscience Inc., Reno, NV, U.S.A.

SUMMARY

Magnetotelluric (MT) profiling in northwestern Nevada is used to test hypotheses on the main sources of heat and hydrothermal fluid for the Dixie Valley-Central Nevada Seismic Belt area. The transect reveals families of resistivity structures commonly dominated by steeply-dipping features, some of which may be of key geothermal significance. Most notably, 2-D inversion of these data has resolved a high-angle, conductive fault zone-like structure extending from the base of Dixie Valley to a broad, deep crustal conductor beneath the Stillwater-Humboldt Range area. The deep conductor is coincident with the Buena Vista anomalous seismic area, and such conductors are generally correlated with magmatic underplating and fluid exsolution. This deeply extending, steep fault zone may be the means for deep transport of fluids upward to provide high temperatures at the Dixie Valley field, including a component of magmatic fluids consistent with recent He isotope studies and the existence of hot springs manifestations in the center of the valley. Decomposed impedance axis analysis suggests the overall trend of this break is nearly N-S. However, other important conductivity structures imaged in the transect include possible large-scale sedimentary folds in the Phanerozoic continental shelf section, and overthrusting near the margin with the Sierra Nevada plutonic province. This experience highlights the need to bring external constraints when interpreting resistivity in the Great Basin.

Wannamaker, P., Hasterok, D., and Doerner, W., 2006. Possible magmatic input to the Dixie Valley geothermal field, Nevada, USA, with implications for district-scale resource exploration, inferred from MT surveying. Proceedings of the 18th IAGA WG 1.2 Workshop on Electromagnetic Induction in the Earth, September 17-23, 2006, El Vendrell, 1-6.

Keywords: Basin and Range, Dixie Valley, Magnetotellurics, Magmatic, Hydrothermal

INTRODUCTION

The Dixie Valley power producing thermal area is a classic, high temperature extensional geothermal system of the Great Basin. However, it lacks nearby young volcanic rocks, and thus is argued to be controlled by large-scale convective fluid flow mining ambient heat from the rock (Benoit, 1999; Blackwell et al., 2000). This is not inconsistent with the area being one of active extension and large historic earthquakes (e.g., Hammond and Thatcher, 2005), but if so, circulation scales must extend to the middle crust at least in order to achieve measured wellbore temperatures ~280 C in the upper 3 km with typical geothermal gradients (McKenna and Blackwell, 2004; Wisian and Blackwell, 2004). In detail however, such circulation models so far have

yielded shallow temperatures only around half the observed. Moreover, seismic and geochemical evidence we will review suggest that cryptic magmatic activity in the crust may not be distant and could influence the hydrothermal regime. In this work, we attempt to trace the reaches of high-T fluid pathways and their sources in the Dixie Valley region and northwestern Great Basin through their influence on electrical resistivity based on a detailed magnetotelluric (MT) profile (Figure 1).

MT DATA COLLECTION AND MODELING

Our MT transect of ~140 soundings is centered on Dixie Valley and oriented WNW-ESE approximately normal to the average trend of horst-graben morphology from the California border in the Smoke

Creek area to near the town of Eureka in central Nevada. In the Dixie Valley area, the line passes through Cottonwood Canyon and the power producing area. About 20 of the five-channel tensor sites were acquired with the University of Utah system, while the remainder were contracted to Quantec Geoscience Inc. Most of the latter were recorded using Reftek data loggers with incorporated in-house electric field preamps and analog signals from EMI Inc. BF4 and BF7 magnetic induction coils. Cross-site remote referencing was standard and, in the western part of the survey, H-fields of the Parkfield California MT observatory were used as references to counteract the Bonneville Power Authority interstate DC power transmission line as it passes through this area (Wannamaker et al., 2004).

Pseudosections of the observed MT responses were presented by Wannamaker et al (2006) and will not be repeated here. However, key features worth noting include alternating high and low apparent resistivity (ρ_a) contours indicative of individual horsts and grabens, and a series of semi-regional highs in the impedance phase (φ) over the 10-100 s band. The latter, particularly evident in the Seven Troughs Range area, from I-80 to Buena Vista Valley, and from the Simpson Park Range to Eureka, will be shown to represent enhanced electrical conductivity in the lower crust. Some of the lateral transitions in the transverse magnetic (TM) mode phase are quite abrupt even though they occur at relatively long periods. The most notable example of these was below central Dixie Valley itself. As reviewed by Wannamaker et al (2006), these abrupt changes are typically associated with steep, crustal scale conducting elements like fault zones connecting electrical currents induced in conductive upper crustal heterogeneity, with large-scale conductors in the deep crust.

An estimate of the strike of the crustal-scale structure beneath our profile was obtained using the phase tensor ellipse method of Caldwell et al. (2004) for the period range 10-400 s. The profile data were grouped into 5 ensembles along the profile and the phase ellipse principal axes plotted in rose histograms, and the average axes and standard deviations computed (Figure 2). A rather clear dominant trend somewhat east of north appears, suggesting that deep structural controls are close to parallel to the surface horst-graben morphology. One possible exception is the trend in the Dixie Valley-Stillwater Range itself, where the trend is more N-S or perhaps a bit west of north. This anomaly in trend may be related to the enhanced crustal permeability which permits the exploitable geothermal systems of Dixie Valley and others to the north and south.

Non-linear 2-D inversion was carried out of the TM mode apparent resistivity and impedance phase, plus the TE vertical magnetic field; these data subsets are relatively robust to finite strike (3-D) effects (Wannamaker, 1999; Ledo et al., 2005) (Figure 3). We used the University of Utah/EGI finite element algorithm implementing an explicit Gauss-Newton parameter step (Wannamaker et al., 1987; DeLugao and Wannamaker, 1996; Tarantola, 1987). The program seeks to fit the data subject to stabilization by adherence to an a-priori model in a first spatial derivative sense. The 1-D starting and a-priori model is shown as a column to the left of the sections, and was derived by integrating the TM mode impedance along the transect (Wannamaker et al., 1997) and performing a smooth 1-D inversion of that sounding. Error floors of $1.5 \log_{10} \%$ in ρ_a , 1° in φ , and 0.015 in vertical H-field were set and RMS misfit is ~ 3.6 .

Numerous heterogeneous features have formed in the model section from the 1-D initial guess (Figure 3). Large low resistivity zones in the lower crust are seen under the Humboldt-Stillwater Range corridor, and under the Simpson Park to Antelope Range area, with lesser ones under the Kumiva-Seven Troughs Ranges and the Clan Alpine-Shoshone Ranges. At the east end of the Stillwater deep conductor, a slablike low resistivity zone dips steeply upward to connect to the bottom of Dixie Valley. Its presence allows simulation of the abrupt change in impedance phase across the center of the valley in the 10-300 s period range and is a robust feature. It does not attach near the range front but rather the center of the valley, where the data break actually occurs (Wannamaker et al., 2006). Additional prominent mid-crustal conductors include one dipping west under the Seven Troughs Range, and other concave-up conductors under the Shoshone and Simpson Park Ranges. Note, however, that several mid-crustal zones of resistivity much higher than the starting model also exist. The lower crustal conductive zones which generally lie in the 15-35 km depth range under most of the line are replaced at the far northwest end by a weaker conductor in the 45-65 km range consistent with a lesser, longer period TM mode phase response. Resistivity variations elsewhere in the uppermost mantle are weak, but this is reaching the limits of penetration of the data in the measured period range. Nevertheless, the uppermost mantle resistivities are considerably larger than those of the lower crust, averaging ~ 60 ohm-m.

PHYSICAL SIGNIFICANCE OF MODEL RESISTIVITY STRUCTURE

The concentrated low resistivity zones of the lower crust of Figure 3, in light of the probable average geotherm of Great Basin crust (Lachenbruch and

Sass, 1978), most likely represent partial melts near the Moho (~900 C near 35 km depth) and high-temperature hypersaline brines (presumably exsolved from said magmas) near their tops (~500 C near 20 km depth) (Wannamaker et al., 1997; Wannamaker, 2000). The most pronounced zone is that extending from the Stillwater Range northwestward nearly to the Trinity Range. It shallows to as little as 15 km below the western Humboldt Range and Interstate Highway 80. The low resistivity zone is roughly coincident with the region of highest seismic reflectivity, the greatest thickness of high V_p (7.4-7.5 km/s) lower crust, and high P-wave amplitude attenuation in the 1986 Nevada PASSCAL wide-angle seismic experiment, all characteristics which have been correlated with magmatic underplating (Catchings and Mooney, 1991). Moreover, the area from Dixie Valley westward is one of enhanced active extension based on modern GPS geodesy (Hammond and Thatcher, 2005), a process known to induce mantle upwelling and partial melting.

A minor additional low resistivity zone in the deep crust lies between the Clan Alpine and Shoshone Ranges, but a surprisingly substantial one is seen under the easternmost end of the line toward Eureka (Figure 3). If this is an area of magmatic underplating also, it implies substantial decoupling between upper mantle processes and those of the crust above in this otherwise stable block (Lowry and Smith, 2000). It would be interesting to follow this conductor to the east to see if it closes, or instead joins with even higher degrees of conductivity in the lower crust of the active eastern Great Basin (Wannamaker et al., 1997). At the west end of the line, the drop in depth of the conductor to 50 km signifies crossing onto rigid, undeformed thick crust of Sierra Nevada affinity, in keeping with the composition of outcrop (e.g., Stewart and Carlson, 1978), but in contrast to the inferred delaminated mantle lid and thinned state of the crust in the southern Sierra Nevada (Ducea, 2001; Park and Wernicke, 2003). The lower crustal conductor is punctured or reduced several times along the profile by restricted areas of high resistivity, such as below the Toiyabe Range and deep below Dixie Valley. We suggest that these are competent bodies of Late Mesozoic or Middle Cenozoic plutonics, mechanically resistant to modern magmatic penetration, based on following the resistors to outcrop. An upper mantle resistivity of 60 ohm-m implies a temperature near 1500 C for dry lherzolite (Duba and Constable 1993). This is far greater than the ~1300 C implied from seismic tomography (Goes and vander Lee, 2002), suggesting the presence of small volume partial melt or hydration to reduce resistivity.

The slablike low resistivity zone dipping steeply upward to connect to the bottom of Dixie Valley from the east end of the Stillwater deep conductor is suggested to be a deep conduit for high temperature fluids exploited at the Dixie Valley system. These fluids appear to intersect the valley at its center, and then ascend along the range-front faulting on the valley's west side. This geometry helps explain the presence of thermal occurrences in the valley center such as Hyder hot springs (Benoit, 1999; Blackwell et al., 2000). We point out that this deep hydrothermal process has 'lit up' Dixie Valley from a low resistivity standpoint in a unique fashion relative to other valleys on the transect, first observed in the dense array surveying of Wannamaker (2003). The proposed conduit connecting the Dixie Valley system with active magmatic underplating nearby to the west could explain the observed elevated He^3 values in Dixie Valley thermal waters (Kennedy and van Soest, 2006). These are generally taken to imply a mantle magmatic component to the waters even though Dixie Valley has been argued to be a deep circulation rather than a magmatic system (McKenna and Blackwell, 2004; Wisian and Blackwell, 2004). Our imaged geometry suggests a means of injecting lower crustal, very high temperature fluids to shallow levels to mix with deep circulation waters.

The large earthquakes of the Central Nevada Seismic Belt (CNSB) (Wesnousky et al., 2005) lie 10-30 km off profile but project near the east transition of the conductive break to localized high resistivity, inferred plutonics. Worldwide, active earthquakes commonly are seen at transitions between conductive and resistive rock, or somewhat within the latter. Such locations are interpreted to allow stress buildup to significant levels before failure, possibly aided by fluid infiltration from the nearby good conductors (reviewed by Wannamaker et al., 2006). At larger scales, this low resistivity crustal break, the major earthquakes, and the CNSB overall coincide with the transition between cratonic Proterozoic North American basement and the Paleozoic accreted terranes under western Nevada (Speed et al., 1988; Burchfiel et al., 1992). Nevertheless, it is difficult to define just how persistent this deep structure is offline. Whether, for example, this crustal break relates to the north more closely with the Beowawe system, or the Grass Valley system, or others in between, would best be settled by parallel profiles of new soundings.

The two concave-up conductors under the Shoshone and Simpson Park Ranges (Figure 3) may reflect processes other than geothermal ones. They roughly flank the Toiyabe uplift, a plutonic-cored N-S trending axis of high metamorphic grade rocks

arising in Late Mesozoic-Middle Cenozoic time (Speed, 1988; Stockli, 1999), and may represent deformed, graphite-bearing conductive strata deep in the Phanerozoic continental shelf section which has been downwarped along the uplift flanks. On the other hand, it is possible that these conductors too represent large-scale, fluidized normal faults of crustal scale. The west-dipping conductive zone starting on the east flank of the Seven Troughs Range (Figure 3) may bear some relation to the middle Miocene epithermal gold deposits there (Hudson et al., 2005), but the dip also is suggestive of control by the mega-scale Late Mesozoic overthrusting of Sierran rocks conjectured to have occurred in the westernmost Great Basin area (Ducea, 2001). The San Emidio geothermal system lies near the junction of the thick Sierran block with the extending Great Basin crust. Hammond and Hatcher (2005) argue for a diffuse axis of enhanced extension in this general area, 75-100 km NW of the CNSB, based on GPS geodetic data.

CONCLUSIONS

We see two main contributions from collection and interpretation of the transect data in this paper. First, a particular electrical structure has been identified which possibly represents a deep hydrothermal source for the Dixie Valley system. It is interpreted to connect to active extension and magmatic underplating in the lower crust. Magmatic underplating is variably concentrated in space in the western Great Basin, and on occasion the related lower crustal conductor seems completely absent in possibly resistant lithologies. Second, long transects such as this provide an opportunity to recognize the breadth of possibilities for creating enhanced conductivity in the crust. This important information underscores the value of external constraints for resistivity models in order to identify the structures which most likely pertain to geothermal processes. It would be interesting to pursue additional profiling parallel to this transect (though of shorter length possibly) in order to trace the Dixie Valley source structure to the northeast or southwest. Further insights could be expected from lengthening the main profile somewhat to increase confidence in the identification of resistivity structural causes and to test for coupling between ultimate deep magmatic sources and upper crustal extension.

ACKNOWLEDGEMENTS

The magnetotelluric data collection, inversion tools, and analysis of this transect have been ongoing efforts under U.S. Dept. of Energy contracts DE-AC07-95ID13274, DE-PS07-00ID13891, DE-FG07-02ID14416 and DE-FG36-04GO14297. The

competence and diligence of the field crew of Quantec Geoscience, principally Jon Powell, Joel Cross, Bruce Frantti and Claudia Moraga, made results of this quality possible. Valuable discussions on resistivity structure and seismicity were held with Marty Unsworth.

REFERENCES

- Benoit, R., 1999, Conceptual models of the Dixie Valley, Nevada geothermal system, *Geothermal Resources Council Transactions*, 23, 505-511.
- Blackwell, D. D., Golan, B., and Benoit, D., 2000, Thermal regime in the Dixie Valley geothermal system, *Proc. World Geothermal Congress, Kyushu, Japan*, 991-996.
- Burchfiel, B. C., Cowan, D. S., and Davis, G. A., 1992, Tectonic overview of the Cordilleran orogen in the western United States, *in* *The Cordilleran orogen: coterminous U. S.*, ed. by B. C. Burchfiel, P. W. Lipman, and M. L. Zoback, *The Geology of North America*, G-3, Geological Society of America, Boulder, 407-480.
- Caskey, S. J., and Ramelli, A. R., 2004, Tectonic displacement and far-field isostatic flexure of pluvial lake shorelines, Dixie Valley, Nevada, *J. Geodynamics*, 38, 131-145.
- Duba, A., and S. Constable, 1993, The electrical conductivity of lherzolite, *J. Geophys. Res.*, 98, 11,885-11,899.
- Ducea, M. N., 2001, The California arc: thick granitic batholiths, eclogitic residues, lithospheric-scale thrusting, and magmatic flare-ups, *Geological Society of America Today*, 11, 4-10.
- DeLugao, P. P., and Wannamaker, P. E., 1996, Calculating the two-dimensional magnetotelluric Jacobian in finite elements using reciprocity, *Geophysical Journal International*, 127, 806-810.
- Goes, S., and van der Lee, S., 2002, Thermal structure of the North American uppermost mantle inferred from seismic tomography, *Journ. Geop. Res.*, 107 (B3), 10.1029/2000JB000049.
- Hammond, W. C., and Thatcher, W., 2005, Northwest Basin and Range tectonic deformation observed with the Global Positioning System, *Journal of Geophysical Research*, 110, JB003678.
- Hudson, D. M., John, D. A., and Fleck, R. J., 2005, Geologic setting, geochemistry, and geochronology of epithermal gold-silver deposits in the Seven

Troughs district, northwest Nevada, Geological Society of America Annual Meeting, paper 166-8, Salt Lake City, Oct. 16-19.

Johnson, S. D., and Hulen, J. B., 2002, Subsurface stratigraphy, structure, and alteration in the Senator thermal area, northern Dixie Valley geothermal field, Nevada – initial results from injection well 38-32, and a new structural scenario for the Stillwater escarpment, Geothermal Resources Council Transactions, 26, 533-542.

Kennedy, B. M., and van Soest, M., 2006, A helium isotope perspective on the Dixie Valley, Nevada, hydrothermal system, Geothermics, 35, 26-43.

Lachenbruch, A. H., and Sass, J. H., 1978, Models of an extending lithosphere and heat flow in the Basin and Range province, *in* Cenozoic tectonics and regional geophysics of the western Cordillera, ed. by R. B. Smith, and G. P. Eaton, Geological Society of America Memoir 152, Boulder, 209-250.

Ledo, J., 2005, 2-D versus 3-D magnetotelluric data interpretation, Surveys in Geophysics, 26, 511-543.

Lowry, A. R., Ribe, N. M., and Smith, R. B., 2000, Dynamic elevation of the Cordillera, western United States, Journal of Geophysical Research, 105, 23,371-23,390.

McKenna, J. R., and Blackwell, D. D., 2004, Numerical modeling of transient Basin and Range extensional geothermal systems, Geothermics, 33, 457-476.

Park, S. K., and Wernicke, B., 2003, Electrical conductivity images of Quaternary faults and Tertiary detachments in the California Basin and Range, Tectonics, 22, 1030, doi: 10.1029/2001TC001324.

Speed, R., Elison, M. W., and Heck, F. R., 1988, Phanerozoic tectonic evolution of the Great Basin”, *in* Metamorphism and crustal evolution of the Western United States, ed. by W. G. Ernst, Rubey volume VII, Prentice-Hall, Englewood Cliffs, NJ, 572-605.

Stewart, J. H., and Carlson, J. E., 1978, Geologic map of Nevada, United States Geological Survey, Reston, 1:500,000 scale.

Stockli, D. F., 1999, Regional timing and spatial distribution of Miocene extension in the northern Basin and Range province, Ph.D. thesis, Stanford University, 239 p.

Tarantola, A., 1987. Inverse problem theory, Elsevier, New York, 671 pp.

Torres-Verdin, C., and Bostick, F. X., Jr., 1992, Principles of spatial surface electric field filtering in magnetotellurics: electromagnetic array profiling (EMAP), Geophysics, 57, 603-622.

Wannamaker, P. E., 1999, Affordable magnetotellurics: interpretation in natural environments, *in* Three-dimensional electromagnetics, ed. by M. Oristaglio and B. Spies, Geophysical Development Series 7, Society of Exploration Geophysics, Tulsa, 349-374.

Wannamaker, P. E., 2000, Comment on ‘The petrologic case for a dry lower crust’, by B. D. Yardley and J. W. Valley, Journal of Geophysical Research, 105, 6057-6064.

Wannamaker, P. E., 2003, Initial Results of Magnetotelluric Array Surveying at the Dixie Valley Geothermal Area, with Implications for Structural Controls and Hydrothermal Alteration, Geothermal Resources Council Transactions, 27, 37-42.

Wannamaker, P. E., Stodt, J. A., and Rijo, L., 1987, A stable finite element solution for two-dimensional magnetotelluric modeling, Geophysical Journal of the Royal Astronomical Society, 88, 277-296.

Wannamaker, P. E., Doerner, W. M., Stodt, J. A., and Johnston, J. M., 1997, Subdued state of tectonism of the Great Basin interior relative to its eastern margin based on deep resistivity structure, Earth and Planetary Science Letters, 150, 41-53.

Wannamaker, P. E., Rose, P. E., Doerner, W. M., Berard, B. C., McCulloch, J., and Nurse, K., 2004, Magnetotelluric surveying and monitoring at the Coso geothermal area, California, in support of the Enhanced Geothermal Systems concept: survey parameters and initial results, Proceedings of the Workshop on Geothermal Reservoir Engineering, Stanford Univ., Stanford, CA, SGP-TR-175, 8 pp.

Wesnousky, S. G., Barron, A. D., Briggs, R. W., Caskey, S. J., Kumar, S., and Owen, L., 2005, Paleoseismic transect across the northern Great Basin, Journal of Geophysical Research, 110, doi:10.1029/2004JB003283.

Wisian, K. W., and Blackwell, D. D., 2004, Numerical modeling of Basin and Range geothermal systems, Geothermics, 33, 713-741.

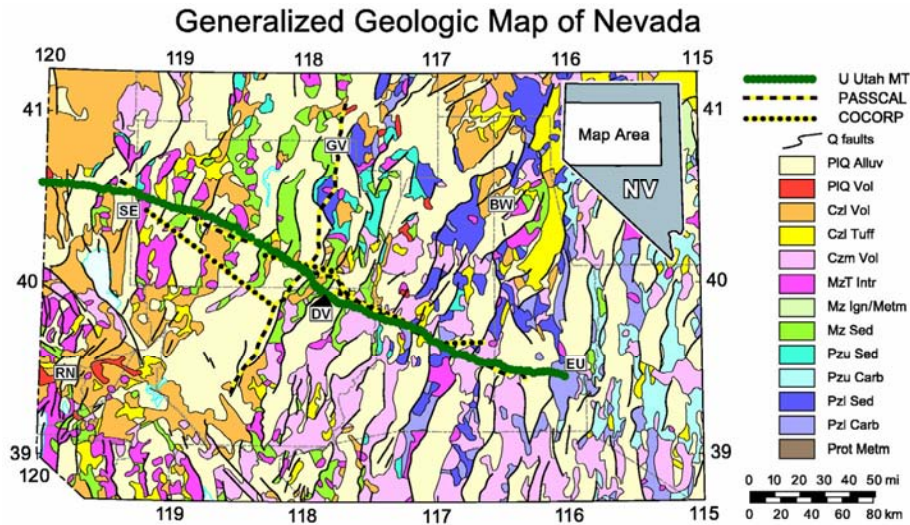


Figure 1. Generalized geological map of northwestern Nevada showing MT station transect and active source seismic profiles of the COCORP and PASSCAL experiments. Locations include Dixie Valley (DV), Reno (RN), Grass Valley (GV), San Emidio (SE), Beowawe (BW) and Eureka (EU).

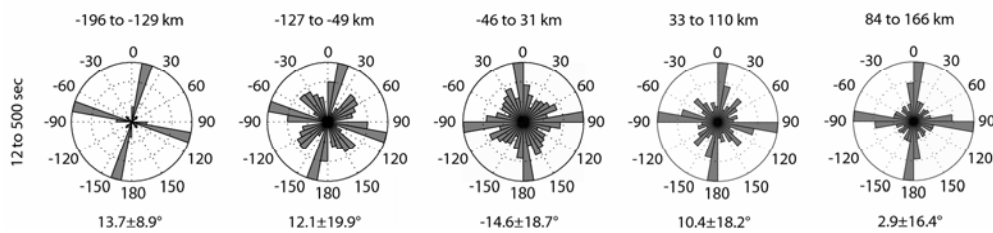


Figure 2. Phase tensor principal axes binned to 10° increments for five length intervals along the transect from west (left) to east (right). Mean direction from true north with s.d. plotted at bottom for each.

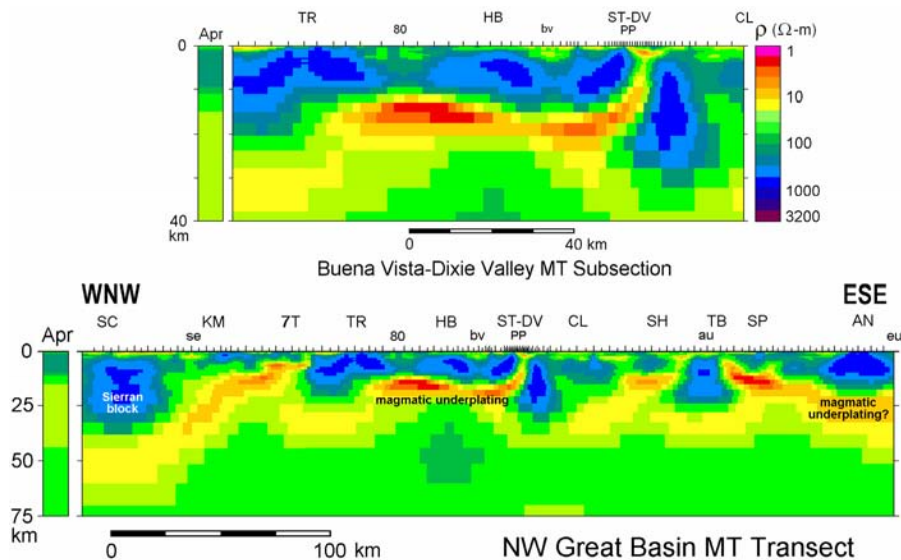


Figure 3. 2-D inversion of MT transect with blow-up of section across Dixie Valley and the Buena Vista anomalous seismic area. Landmarks include Smoke Creek (SC), San Emidio hot springs, (se), Kumiva Peak (KM), Seven Troughs Range (7T), Trinity Range (TR), I-80, Humboldt Range (HB), Buena Vista Valley (bv), Stillwater Range-Dixie Valley system (ST-DV), power plant (PP), Clan Alpine Range (CL), Shoshone Range (SH), town of Austin (au), Toiyabe Range (TB), Simpson Park Range (SP), Antelope Range (AN), and town of Eureka (eu).